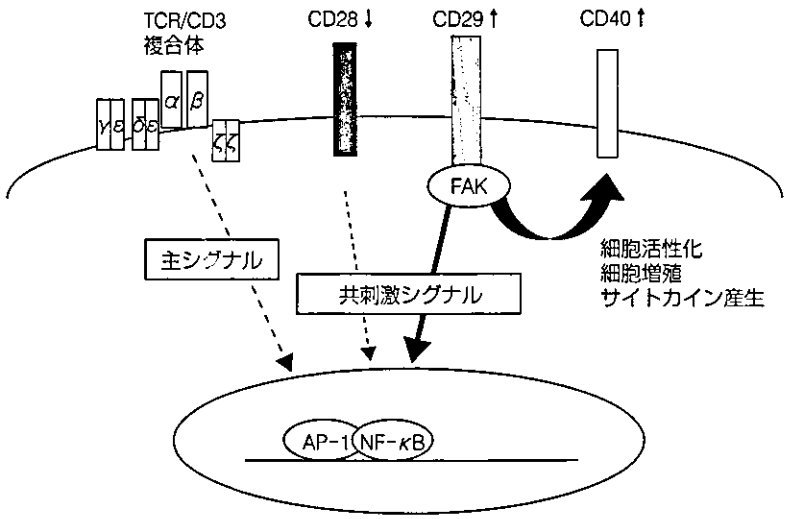

図 4. SLE 患者 T 細胞活性化における CD 28 の減弱に対する β_1 インテグリンの相補的役割
活動期 SLE 患者 T 細胞では，CD 28 の低下に反比例して，β_1 インテグリン (CD 29) を介するシグナルが亢進し，さらに，β_1 インテグリン-FAK を介する賦活化シグナルの亢進は，CD 28 非依存性に作用し，自己反応性 T 細胞の過剰な活性化に寄与する．

常の是正を目的として，新規治療軸の確立が期待される．実際，インテグリンの拮抗薬として開発されたヒト化抗 α_4 抗体 natalizumab が中等度から重度のクローン病，および再発性多発性硬化症に対して臨床試験がなされ，すぐれた臨床効果と忍容性が認められ，米国食品医薬品局(Food and Drug Administration：FDA)に承認申請中である[28)29)]．

おわりに

現在，免疫シグナル異常の是正を目的とした病態特異的な新規治療軸の確立が期待されるが，SLE では，CD 40/CD 40 L，B 7 h/ICOS などを介する共刺激分子シグナルが標的分子として注目され，CD 40 L 抗体，BlyS 抗体などの臨床試験が開始されている[7)16)30)]．今回，SLE の T 細胞では，代表的な共刺激分子である CD 28 の減弱に反して，β_1 インテグリン(CD 29)と CD 40 L が増強することを見出した．その機構として，β_1-FAK を介する賦活化シグナルの量的，および，質的な亢進は，従来の T 細胞活性化の経路をバイパスした CD 28 非依存性の共刺激として作用し，CD 40 L などの発現を誘導して自己反応性 T 細胞の過剰な活性化をもたらし，ループス腎炎などの臓器病変の進展を引き起こす可能性が示唆された．癌の化学療法の分野では，チロシンキナーゼや FAK の恒常的活性化を認める白血病や肺癌，乳癌に対して，その阻害薬が分子標的治療薬として試験が先行し，ことに，癌抑制遺伝子 *PTEN* が FAK の活性化を抑制する負の制御機構が注目される[31)]．一方，リンパ球特異的に PTEN を欠損させると，SLE 様の自己免疫疾患の発症，腫瘍化が引き起こされる[32)]．したがって，SLE においても，β_1 インテグリンや FAK に対する阻害薬，さらに，PTEN による制御も魅力的な治療の手法となりうる．

文　献

1) Criscione LG *et al*：B lymphocytes and sys-

temic lupus erythematosus. *Curr Rheumatol Rep* **5**: 264-269, 2003
2) Krishnan S *et al*: T cell rewiring in differentiation and disease. *J Immunol* **171**: 3325-3331, 2003
3) Tanaka Y *et al*: Mechanism of spontaneous activation of B cells in patients with systemic lupus erythematosus. Analysis with anti-class II antibody. *J Immunol* **140**: 761-767, 1988
4) Sakaguchi S: Regulatory T cells: mediating compromises between host and parasite. *Nat Immunol* **4**: 10-11, 2003
5) von Herrath MG *et al*: Antigen-induced regulatory T cells in autoimmunity. *Nat Rev Immunol* **3**: 223-232, 2003
6) Schluns KS *et al*: Cytokine control of memory T-cell development and survival. *Nat Rev Immunol* **3**: 269-279, 2003
7) Tanaka Y *et al*: T-cell adhesion induced by proteoglycan-immobilized cytokine MIP-1 β. *Nature* **361**: 79-82, 1993
8) Nakayamada S *et al*: β_1 integrin-mediated signaling induces intercellular adhesion molecule 1 and Fas on rheumatoid synovial cells and Fas-mediated apoptosis. *Arthritis Rheum* **48**: 1239-1248, 2003
9) Nakayamada S *et al*: β_1 integrin/focal adhesion kinase-mediated signaling induces intercellular adhesion molecule 1 and receptor activator of nuclear factor κB ligand on osteoblasts and osteoclast maturation. *J Biol Chem* **278**: 45368-45374, 2003
10) Kamiguchi K *et al*: Cas-L is required for β_1 integrin-mediated costimulation in human T cells. *J Immunol* **163**: 563-568, 1999
11) Shanahan JC *et al*: Upcoming biologic agents for the treatment of rheumatic diseases. *Curr Opin Rheumatol* **15**: 226-236, 2003
12) Daikh DI *et al*: Long-term inhibition of murine lupus by brief simultaneous blockade of the B 7/CD 28 and CD 40/gp 39 costimulation pathways. *J Immunol* **159**: 3104-3108, 1997
13) Mackay F *et al*: TNF ligands and receptors in autoimmunity: an update. *Curr Opin Immunol* **14**: 783-790, 2002
14) Kalled SL *et al*: B cell survival factor and emerging therapeutic target for autoimmune disorders. *Expert Opin Ther Targets* **7**: 115-123, 2003
15) Ramanujam M *et al*: Polyclonal B cell activation in NZB/W F 1 mice is dependent on B Cell stimulation through TACI/BCMA but not BR -3. *Arthritis Rheum* **48**: S 595, 2003
16) Furie R *et al*: Safety, pharmacokinetic and pharmacodynamic results of a phase 1 single and double dose-escalation study of lymphostat-B (human monoclonal antibody to BLyS) in SLE patients. *Arthritis Rheum* **48**: S 317, 2003
17) Kremer JM *et al*: Treatment of rheumatoid arthritis by selective inhibition of T-cell activation with fusion protein CTLA 4 Ig. *N Engl J Med* **349**: 1907-1915, 2003
18) Horwitz DA *et al*: Decreased T cell response to anti-CD 2 in systemic lupus erythematosus and reversal by anti-CD 28: evidence for impaired T cell-accessory cell interaction. *Arthritis Rheum* **40**: 822-833, 1997
19) Alvarado C *et al*: Effect of CD 28 antibody on T cells from patients with systemic lupus erythematosus. *J Autoimmun* **7**: 763-773, 1994
20) Brinchmann JE *et al*: Expression of costimulatory molecule CD 28 on T cells in human immunodeficiency virus type 1 infection: functional and clinical correlations. *J Infect Dis* **169**: 730-738, 1994
21) Takeuchi T *et al*: Upregulated expression and function of integrin adhesive receptors in systemic lupus erythematosus patients with vasculitis. *J Clin Invest* **92**: 3008-3016, 1993
22) Pallis M *et al*: Correlation between CD 29 density on CD 8+lymphocytes and serum IgG in systemic lupus erythematosus. *Lupus* **6**: 379-384, 1997
23) Ng TT *et al*: Integrin signalling defects in T -lymphocytes in systemic lupus erythematosus. *Lupus* 8: 39-51, 1999
24) Parsons JT: Focal adhesion kinase: the first ten years. *J Cell Sci* **116**: 1409-1416, 2003
25) Kelley VR *et al*: Cytokines in the pathogenesis of systemic lupus erythematosus. *Semin Nephrol* **19**: 57-66, 1999
26) Morino N *et al*: Glomerular overexpression

and increased tyrosine phosphorylation of focal adhesion kinase p125FAK in lupus-prone MRL/MP-lpr/lpr mice. *Immunology* **97**: 634-640, 1999
27) James WG *et al*: Critical role of the alpha 4 integrin/VCAM-1 pathway in cerebral leukocyte trafficking in lupus-prone MRL/fas(lpr) mice. *J Immunol* **170**: 520-527, 2003
28) Ghosh S *et al*: Natalizumab for active Crohn's disease. *N Engl J Med* **348**: 24-32, 2003
29) Miller DH *et al*: A controlled trial of natalizumab for relapsing multiple sclerosis. *N Engl J Med* **348**: 15-23, 2003
30) Boumpas DT *et al*: A short course of BG9588(anti-CD40 ligand antibody)improves serologic activity and decreases hematuria in patients with proliferative lupus glomerulonephritis. *Arthritis Rheum* **48**: 719-727, 2003
31) Tamura M *et al*: Inhibition of cell migration, spreading, and focal adhesions by tumor suppressor PTEN. *Science* **280**: 1614-1617, 1998
32) Suzuki A *et al*: T cell-specific loss of Pten leads to defects in central and peripheral tolerance. *Immunity* **14**: 523-534, 2001

+TAKEUCHI Tsutomu/埼玉医科大学総合医療センター第二内科

THE JOURNAL OF BIOLOGICAL CHEMISTRY
Vol. 279, No. 18, Issue of April 30, pp. 18688–18693, 2004
Printed in U.S.A.

Expression Cloning of a Human cDNA Restoring Sphingomyelin Synthesis and Cell Growth in Sphingomyelin Synthase-defective Lymphoid Cells*

Received for publication, February 3, 2004
Published, JBC Papers in Press, February 19, 2004, DOI 10.1074/jbc.M401205200

Shohei Yamaoka, Michihiko Miyaji, Toshiyuki Kitano‡, Hisanori Umehara, and Toshiro Okazaki§

From the Departments of Hematology/Oncology and Clinical Immunology and the ‡Outpatient Oncology Unit, Graduate School of Medicine, Kyoto University, 54 Shogoin-Kawaharacho, Sakyo-ku, Kyoto 6068507, Japan

Sphingomyelin (SM) synthase has been assumed to be involved in both cell death and survival by regulating pro-apoptotic mediator ceramide and pro-survival mediator diacylglycerol. However, its precise functions are ambiguous due to the lack of molecular cloning of SM synthase gene(s). We isolated WR19L/Fas-SM(−) mouse lymphoid cells, which show a defect of SM at the plasma membrane due to the lack of SM synthase activity and resistance to cell death induced by an SM-directed cytolytic protein lysenin. WR19L/Fas-SM(−) cells were also highly susceptible to methyl-β-cyclodextrin (MβCD) as compared with the WR19L/Fas-SM(+) cells, which are capable of SM synthesis. By expression cloning method using WR19L/Fas-SM(−) cells and MβCD-based selection, we have succeeded in cloning of a human cDNA responsible for SM synthase activity. The cDNA encodes a peptide of 413 amino acids named SMS1 (putative molecular mass, 48.6 kDa), which contains a sterile α motif domain near the N-terminal region and four predicted transmembrane domains. WR19L/Fas-SM(−) cells expressing SMS1 cDNA (WR19L/Fas-SMS1) restored the resistance against MβCD, the accumulation of SM at the plasma membrane, and SM synthesis by transferring phosphocholine from phosphatidylcholine to ceramide. Furthermore, WR19L/Fas-SMS1 cells, as well as WR19L/Fas-SM(−) cells supplemented with exogenous SM, restored cell growth ability in serum-free conditions, where the growth of WR19L/Fas-SM(−) cells was severely inhibited. The results suggest that SMS1 is responsible for SM synthase activity in mammalian cells and plays a critical role in cell growth of mouse lymphoid cells.

Diverse kinds of phospho- and glycerolipids such as diacylglycerol (DAG),[1] inositol phosphatides, and phosphatidic acid are recognized as bioactive molecules in cell growth and survival (1, 2). Sphingolipid ceramide has recently emerged as a signal mediator of cell functions including apoptosis, differentiation, and secretion (3). Various stresses such as ultraviolet, irradiation, heat shock, hypoxia, and biological factors such as tumor necrosis factor-α, interferon-γ, and Fas antibody require ceramide generation to execute apoptosis, suggesting the implications of SM as a source of ceramide generation in the induction of cell death (4, 5). It was reported that SM dose-dependently inhibits both deoxycholate-induced apoptosis and subsequent hyper-proliferation in colon epithelial cells (6) and decreases the number of aberrant crypts of colon (7), suggesting the implications of SM in cell death and growth.

SM is produced by SM synthase, which is thought to be the only enzyme to synthesize SM in mammalian cells (8). The enzyme catalyzes the reaction in which phosphocholine moiety is transferred from phosphatidylcholine (PC) to ceramide. Thus, the activation of SM synthase subsequently increases the levels of DAG and decreases ceramide at the same time (8). DAG is an important signaling molecule for cell growth through protein kinase C activation (9–12) and acts competitively against ceramide-induced apoptosis (4, 13). It has been reported that after thioacetamide-induced injury, the SM/PC ratio significantly increased in microsomal fraction from liver, suggesting the involvement of SM synthase in tissue recovery (14). In cerebellar astrocytes, the level of ceramide is rapidly down-regulated by basic fibroblast growth factor via activating SM synthase (15). In SV40-transformed lung fibroblasts, SM synthase regulates the levels of ceramide and DAG in an opposite direction (16). We recently reported that SM synthase was activated to inhibit ceramide generation in IL-2-induced proliferation of natural killer cells,[2] whereas the activity in nucleus was inhibited with ceramide generation in Fas-induced T cell apoptosis (17). We also showed its *in vivo* implication that the level of ceramide was decreased via activation of SM synthase in chemotherapy-resistant blast cells obtained from refractory leukemia patients than in chemotherapy-sensitive leukemic blasts (18). Thus, SM synthase is assumed to play an important role in cell death and survival, *in vitro* as well as *in vivo*.

We previously proposed the "SM cycle," a pathway that consisted of SM synthase and sphingomyelinase as a novel biological system to regulate the cellular level of ceramide for cell death and differentiation (19). In contrast to the studies of the acid and neutral sphingomyelinases in cell death (20, 21), the biological implication of SM synthase has not been elucidated due to the lack of molecular cloning of its responsible gene(s).

* This work was supported by a grant from the Ministry of Education, Culture, Sports, Science and Technology of Japan (MEXT). The costs of publication of this article were defrayed in part by the payment of page charges. This article must therefore be hereby marked "*advertisement*" in accordance with 18 U.S.C. Section 1734 solely to indicate this fact.

The nucleotide sequence(s) reported in this paper has been submitted to the GenBank™/EBI Data Bank with accession number(s) AB154421.

§ To whom correspondence should be addressed. Tel. and Fax: 81-75-751-3154; E-mail: toshiroo@kuhp.kyoto-u.ac.jp.

[1] The abbreviations used are: DAG, diacylglycerol; SM, sphingomyelin; PC, phosphatidylcholine; MβCD, methyl-β-cyclodextrin; SAM, sterile α motif; WST-8, 2-(2-methoxy-4-nitrophenyl)-3-(4-nitrophenyl)-5-(2,4-disulfophenyl)-2H-tetrazolium; FBS, fetal bovine serum; FACS, fluorescence-activated cell sorter; MBP, maltose-binding protein; NBD, 12-(*N*-methyl-*N*-(7-nitrobenz-2-oxa-1,3-diazol-4-yl)).

[2] Y. Taguchi, T. Kondo, M. Watanabe, Y. Kozutumi, and T. Okazaki, submitted for publication.

We recently found mouse lymphoid cell variants designated WR19L/Fas-SM(−), which are defective of SM synthesis and susceptible to methyl-β-cyclodextrin (MβCD)-induced cell death (30). By an expression cloning method using WR19L/Fas-SM(−) cells and MβCD-based cell selection, we isolated a human cDNA responsible for SM synthase activity. The cDNA clone encodes a peptide of 413 amino acids, named SMS1, which contains a sterile α motif (SAM) domain and four putative transmembrane domains. SMS1 was identical to the peptide that was recently identified as a human SM synthase by Huitema *et al.* (24). In serum-free condition, where the cell growth of WR19L/Fas-SM(−) was inhibited, the cells expressing SMS1 cDNA (WR19L/Fas-SMS1) restored the growth ability and accumulation of SM at the surface of the plasma membrane. The restoration of cell growth was also observed when WR19L/Fas-SM(−) cells were maintained in the serum-free medium supplemented with exogenous SM. Here, we show the critical role of SM synthesized through SM synthase in mammalian cell growth, and the localization, active site and biological function of SMS1 are also discussed.

EXPERIMENTAL PROCEDURES

Materials—Lysenin, MβCD, and ceramide from bovine brain were purchased from Sigma; PC from egg yolk, SM from bovine brain, and a cell viability assay kit with 2-(2-methoxy-4-nitrophenyl)-3-(4-nitrophenyl)-5-(2,4-disulfophenyl)-2H-tetrazolium (WST-8) were from Nacalai tesque (Kyoto, Japan); GP2-293 packaging cell, pLIB retroviral expression vector, and human HeLa cDNA retroviral expression library were from Clontech; D-erythro-C6-NBD-ceramide and C6-NBD-sphingomyelin were from Matreya (Pleasant Gap, PA); L-[U-^{14}C]serine, cytidine 5′-diphospho [methyl-^{14}C]choline, L-3-phosphatidyl [N-methyl-^{14}C]choline, 1,2-dipalmitoyl, and [N-methyl-^{14}C]sphingomyelin were from Amersham Biosciences.

Cell Culture—WR19L/Fas cells were kindly gifted from Dr. Yonehara (Institute for Virus Research, Kyoto University). The SM-defective WR19L/Fas-SM(−) cells and the SM-containing WR19L/Fas-SM(+) cells were isolated from the original WR19L/Fas cells by a dilution cloning method. The cells were routinely maintained in RPMI 1640 medium supplemented with 10% fetal bovine serum (FBS), 50 μM 2-mercaptoethanol, and 75 μg/ml kanamycin in 5% CO_2 and 100% humidity at 37 °C. For culture in serum-free medium, the cells were washed, reseeded at 1×10^5 cells/ml, and incubated in the RPMI 1640 medium with 5 μg/ml human insulin and bovine holo transferrin in the presence or absence of 50 μM SM in 5% CO_2 at 37 °C. After 48 h incubation, the cell numbers were counted with dye exclusion method using 0.25% trypan blue (Nakalai tesque, Kyoto, Japan).

Cell Labeling—The cells were reseeded at 5×10^5 cells/ml in the RPMI 1640 medium with 2% FBS and L-[^{14}C]serine (specific activity; 155 mCi/mmol) and incubated at 37 °C in 5% CO_2 for 36 h. The labeled cells were incubated at 37 °C in 5% CO_2 for 2 h. The cell lipids were extracted by the method of Bligh and Dyer (19), applied on a silica Gel 60 TLC plate (Merck), and developed with solvent containing methyl acetate/propanol/chloroform/methanol/0.25% KCl (25:25:25:10:9). The radioactive spots were visualized and quantified by using a BAS 2000 Image Analyzer (Fuji Film).

FACS Analyses—The cells were incubated with 500 ng/ml lysenin in the presence of 20 μg/ml propidium iodide (Molecular Probes) at room temperature for 15 min and analyzed with FACS Calibur (BD Biosciences). For detection of SM localized at the plasma membrane, the cells were stained on ice for 30 min with non-toxic lysenin fused to maltose-binding protein (MBP-lysenin) (25), kindly provided by Dr. T. Kobayashi (The Institute of Physical and Chemical Research (RIKEN), Japan). The cells were washed with ice-cold phosphate-buffered saline supplemented with 1% FCS and 0.1% NaN_3 and incubated with rabbit anti-MBP antiserum (New England BioLabs, Beverly, MA) on ice for 30 min. After being washed again, the cells were incubated for 30 min with phycoerythrin-conjugated anti-rabbit IgG (Sigma) and subjected to fluorescence-activating cell sorter (FACS) analysis using FACS Calibur. The data analysis was performed by Cell Quest software (BD Biosciences).

Confocal Microscopy—For visualization of SM localized at the plasma membrane, the cells settled onto slides coated with poly-L-lysine were fixed in 4% formaldehyde and stained with lysenine-MBP at 4 °C for 45 min followed with anti-MBP. After being stained with a phycoerythrin-conjugated anti-rabbit IgG monoclonal antibody, the cells were examined using confocal microscopy using a Zeiss LSM 310 laser scan confocal microscope (Carl Zeiss, Oberkochen, Germany).

Expression Cloning of SMS1 cDNA—The expression cloning method performed in this study was based on the study of Hanada *et al.* (26). Pantropic retroviral particles containing the G glycoprotein of vesicular stomatitis virus (VSV-G) were prepared using a human HeLa cDNA retroviral expression library kit and GP2-293 packaging cells (Clontech). After infection for 24 h, the WR19L/Fas-SM(−) cells were cultured in the RPMI 1640 medium containing 2% FBS overnight. After being washed with serum-free RPMI 1640 medium, the cells were incubated in 1.5 mM MβCD in RPMI 1640 medium for 5 min at 37 °C, replenished with the normal culture medium to a final concentration of FBS at 5%, and then cultured at 37 °C for 60 h. The cells were reseeded, cultured in the RPMI 1640 medium containing 2% FBS overnight, and subjected again to the treatment with appropriate concentrations of MβCD. After a total of two cycles of 1.5 mM MβCD treatment followed by two cycles of 3 mM and two subsequent cycles of 5 mM, an MβCD-resistant variant of WR19L/SM(−) was isolated by a limiting dilution.

By genomic PCR using primers specific to the pLIB expression vector (5′ and 3′ pLIB Primer, Clontech), the 2.0-kb cDNA integrated in the genome of the MβCD-resistant cell was amplified and cloned into pGEM-T Easy vector (Promega, Madison, WI). After sequencing and computer analysis, the cDNA was subcloned into the pLIB expression vector and transfected into the WR19L/Fas-SM(−) cells via the VSV-G retroviral particles. A resultant cell was isolated by a limiting dilution method, which was designated WR19L/Fas-SMS1 cells, and subjected to various assays. Integration of the cDNA into the genome of WR19L/Fas-SMS1 cells was confirmed with PCR.

Assay for Sphingomyelin Synthase Activity—The cells were homogenized in an ice-cold buffer containing 20 mM Tris-HCl, pH 7.4, 2 mM EDTA, 10 mM EGTA, 1 mM phenylmethylsulfonyl fluoride, and 2.5 μg/ml leupeptin. The lysates containing 500 μg of cell protein were added to a reaction solution containing 10 mM Tris-HCl, pH 7.5, 1 mM EDTA, 20 μM C6-NBD-ceramide, 120 μM PC and incubated at 37 °C for 30 min. The lipids were extracted by the method of Bligh and Dyer (19), applied on the TLC plates, and developed with solvent containing chloroform/methanol/12 mM $MgCl_2$ in H_2O (65:25:4). The fluorescent lipids were visualized by FluorImager SI system (Amersham Biosciences). For the assay for transferase activity, 20 μM ceramide and 120 μM [N-methyl-^{14}C]PC (specific activity; 57 mCi/mmol) or [methyl-^{14}C]CDP-choline (specific activity; 54 mCi/mmol) were used in the reaction solution instead of the NBD-ceramide and PC. The radioactive spots were visualized using the BAS 2000 system.

Assay for Viability and Growth Rate of Cells Exposed to MβCD and Lysenin—For the assay using MβCD, 1×10^6 of the cells were washed and resuspended in 1 ml of the serum-free RPMI 1640 medium, treated with appropriate concentrations of MβCD, and incubated in 5% CO_2 at 37 °C for 5 min. After the addition of 1 ml of the normal culture medium, the cells were further incubated for 12 h. The viability of the cells was measured using a cell viability kit with WST-8 (Nakalai tesque). For the assay using lysenin, 7×10^5 of the cells were washed and resuspended in 1 ml of prewarmed phosphate-buffered saline, treated with the appropriate concentrations of lysenin and incubated in 5% CO_2 at 37 °C for 1 h. After the addition of FBS, the cell number was counted with the 0.25% trypan blue dye exclusion method.

RESULTS AND DISCUSSION

Mouse Lymphoid Cells Defective of Sphingomyelin Synthase Activity—During investigation of the sphingolipid metabolism in mouse lymphoid cells named WR19L/Fas, which overexpress the human Fas antigen, the variant clones altering SM synthase activity (from 150 to nearly 0 pmol/mg protein/h) have been isolated. One of the variants (clone 6) severely diminished the SM synthase activity (Fig. 1*A*). Conversion of C6-NBD-ceramide to C6-NBD-SM in the cell lysate of the clone 6, named WR19L/Fas-SM(−), was not detected on a TLC plate, in contrast to the clone 2 showing the highest SM synthase activity, named WR19L/Fas-SM(+) (Fig. 1*B*). This finding was supported by the fact that WR19L/Fas-SM(−) cells did not synthesize [^{14}C]serine-labeled SM (Fig. 1*C*).

Lysenin is reported as an SM-direct cytolysin purified from the earthworm (27), for which binding to SM causes poring of the plasma membrane and subsequent cell death (22, 23, 25).

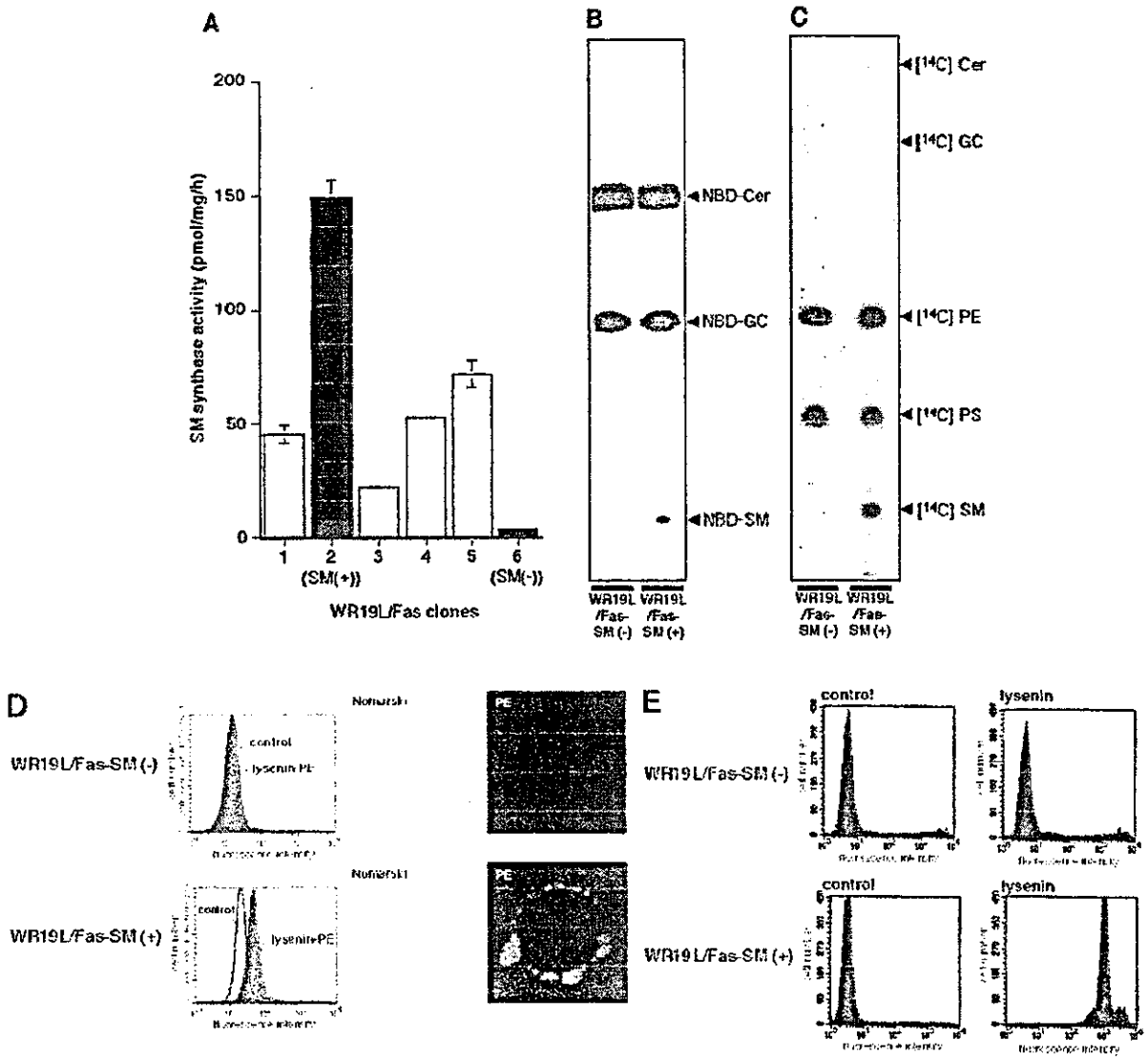

FIG. 1. **Deficiency of SM synthesis, SM synthase activity, and SM localized at the plasma membrane in the WR19L/Fas-SM(−) cells.** *A*, SM synthase activity in the cell lysates of the variant WR19L/Fas cells was assessed by the generation of C6-NBD-SM. The NBD-labeled products were quantified by a fluorospectro-photometer. *B*, SM synthase activity of WR19L/Fas-SM(−) and −SM(+). The NBD-labeled products developed on the TLC plate were visualized by a fluorospectro-photometer. The reaction was performed in the presence of 0.5 mM UDP-glucose. *Cer*, ceramide; *GC*, glucosylceramide; *C*, the cellular lipids were labeled with [^{14}C]serine, extracted by the Bligh and Dyer method, and assessed by TLC. The radiolabeled products developed on the TLC plate were visualized by BAS 2000 system. *PE*, phosphatidylethanolamine; *PS*, phosphatidylserine. *D*, SM localized at the plasma membrane was assessed by FACS analysis and confocal microscopy. FACS analysis was performed for the cells treated with the MBP-conjugated modified lysenin (*shaded* with *dark blue*) and the control cells (*unshaded*). For the results of the confocal microscopy, the fluorescence of phycoerythrin (*PE*) was pseudo-colored with *red*. *E*, The cells stained with 500 ng/ml lysenin in the presense of 20 μg/ml propidium iodide were assessed by FACS analysis. The data were the average and 1 S.D. obtained from three independent experiments (*A*) and were the representative of three independent experiments (*B–E*).

Hanada *et al.* (22) previously showed that Chinese hamster ovary cells, which express SM in the outer surface of the plasma membrane, were sensitive to lysenin-induced cell death. They also showed that reduced accumulation of SM in the variant Chinese hamster ovary cells, LY-A and LY-B, causes the significant resistance against lysenin (22). In LY-A cells, the reduction of SM is caused by the lack of non-vesicular transporter for ceramide between endoplasmic reticulum (ER) and Golgi apparatus (CERT) (26), whereas in LY-B cells, it is due to the lack of LCB1, a component of serine palmitoyltransferase (22). CERT is involved in SM synthesis by transferring ceramide from the endoplasmic reticulum to the cytoplasmic surface of Golgi apparatus (26, 31). Recently, Kobayashi and co-workers (25) reported a modified lysenin, which specifically binds to SM without the induction of cell death. By using the modified lysenin conjugated with MBP, we examined the accumulation of SM on the cellular surface of WR19L/Fas-SM(−) cells. Binding of the modified lysenin was positively detected in WR19L/Fas-SM(+) cells but not in WR19L/Fas-SM(−) cells by FACS analysis and confocal microscopy using anti-MBP antibody (Fig. 1*D*), indicating that the accumulation of SM on the outer surface of the WR19L/Fas-SM(−) cells was severely reduced. The results were supported by the fact that WR19L/Fas-SM(+) cells underwent cell death by treatment with the cytotoxic lysenin, whereas WR19L/Fas-SM(−) cells did not, when we examined cell viability by staining with propidium iodide and subsequent FACS analysis (Fig. 1*E*). These facts suggest that the severe reduction of SM at the cellular surface of WR19L/Fas-SM(−) cells is due to the lack of enzymatic activity of SM synthase.

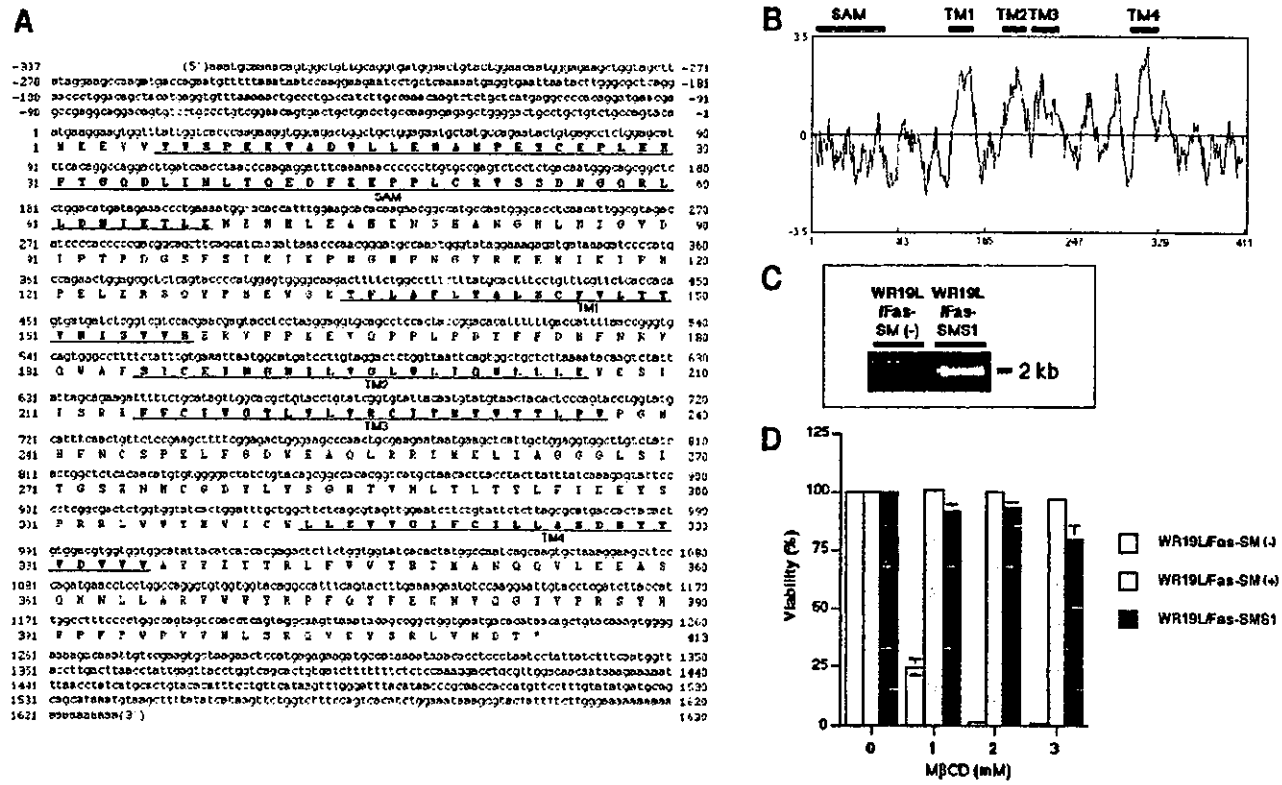

FIG. 2. **Expression cloning of a human cDNA responsible for cellular resistance to methyl-β-cyclodextrin.** *A*, nucleotide sequence and predicted amino acid sequence of SMS1. Putative SAM domain sequence and transmembrane (*TM*) regions are indicated with the *thin* and *thick underline*, respectively. SAM domain and transmembrane domains were predicted by the BLAST algorithm and SOSUI program, respectively. *B*, hydropathy plot of the amino acid sequence of SMS1 analyzed by the method of Kyte and Doolittle (45). Positions of the putative SAM domain and transmembrane regions are indicated with *horizontal bars*. *C*, integration of SMS1 cDNA (2 kb) into the genome of WR19L/Fas-SM(−) and −SMS1 cells was examined by PCR. *D*, the viability of WR19L/Fas-SM(−), −SM(+), and −SMS1 cells exposed to various concentrations of MβCD. The viability of the cells was examined using WST-8. The data were the average and 1 S.D. obtained from three independent experiments.

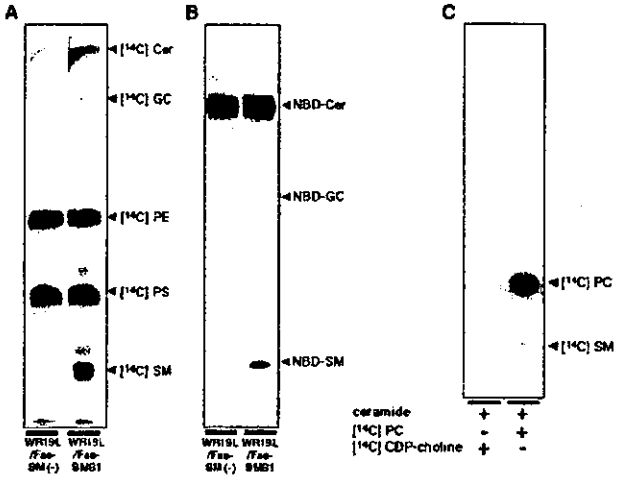

FIG. 3. **Restoration of SM synthesis and SM synthase activity in WR19L/Fas-SMS1.** *A*, the cellular lipids of WR19L/Fas-SM(−) and −SMS1 labeled with [^{14}C]serine were assessed by TLC as described in Fig. 1. *Cer*, ceramide; *GC*, glucosylceramide; *PE*, phosphatidylethanolamine; *PS*, phosphatidylserine. *B*, SM synthase activity of WR19L/Fas-SM(−) and −SMS1 cells was assessed in the absence of UDP-glucose as described in the legend for Fig. 1. *C*, SM synthase activity was assessed using the radiolabeled PC and CDP-choline as the donor of phosphocholine moiety. The radiolabeled products developed on the TLC plate were visualized by BAS 2000 system. The data were the representative of three independent experiments.

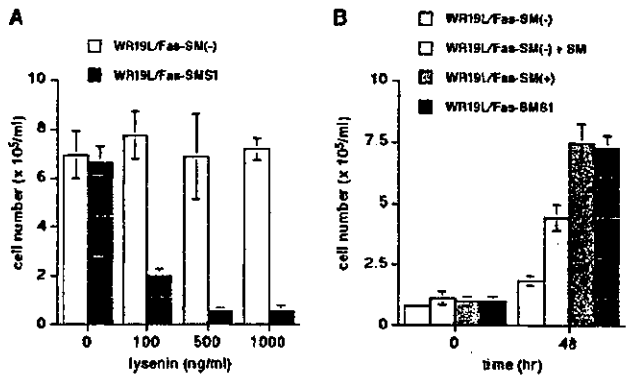

FIG. 4. **The SMS1 cDNA is essential for normal growth in mammalian lymphoid cells.** *A*, a viability assay of the WR19L/Fas-SM(−) and −SMS1 cells exposed to lysenin. After treatment with the indicated concentrations of lysenin at 37 °C for 1 h, the cell numbers were assessed by the dye exclusion method. *B*, growth of WR19L/Fas-SM(−), −SM(+), and −SMS1 cells in serum-free medium and restoration of WR19L/Fas-SM(−) cell growth by supplement of SM. The cells were incubated in serum-free medium for 48 h in the presence or absence of 50 μM SM, and the cell numbers were assessed by the dye exclusion method. The data were the average and 1 S.D. obtained from three independent experiments.

Expression Cloning of a Human cDNA Responsible for Resistance to Methyl-β-cyclodextrin-induced Cell Death—It has been reported that SM strongly interacts with cholesterol in biological and artificial membranes (28) and that SM is required to form the membrane microdomains (lipid rafts) related to cell functions such as cell death and growth (29, 30). LY-A cells were sensitive to MβCD-induced cell death due to the decrease of the SM level in plasma membrane (30). We similarly observed that WR19L/Fas-SM(−) cells were highly

sensitive to MβCD-induced cell death, whereas WR19L/Fas-SM(+) cells were not (Fig. 2*D*). This finding allowed us to screen WR19L/Fas-SM(−) cells complemented with the ability of SM synthesis using MβCD as a selective agent. Using a pantropic retroviral transfection system, WR19L/SM(−) cells were transfected with a cDNA expression library of the human HeLa cell, and the variant cells, which were resistant to MβCD due to the expression of SM in the plasma membrane, were selected. The variant cells were isolated to a single clone by a limiting dilution method. The purified cells integrated a human cDNA of 1967 bp in the genome, which encodes a peptide of 413 amino acids with 48.6 kDa of a predicted molecular mass (Fig. 2*A*). The BLAST algorithm (32) and the SOSUI program (33) suggested that this peptide carries a SAM domain in the N-terminal region and four transmembrane helices, respectively (Fig. 2*B*). The SAM domain is suggested to be involved in signal transduction, development, and transcriptional regulation (34, 35). A variety of proteins such as ephrin-related receptor tyrosine kinase, a variant of p53 (p73), and DAG kinase δ contain the SAM domain(s), which may play a role in protein-protein or protein-lipid interaction (35, 36). Recently, Huitema *et al.* (24) reported a family of SM synthases using a bioinformatics and functional cloning strategy in yeast. They identified the human cDNAs encoding the peptides that shared a sequence motif with the lipid phosphate phosphatases and Aur1p proteins required for inositolphosphorylceramide production in yeast (24). One of the human peptides, SMS1, was identical to our peptide. They further demonstrated that SMS1 was localized at Golgi apparatus and predicted the six transmembrane domains and an exoplasmic catalytic site, which is consistent with the characteristics of SM synthase suggested previously (37–39). Molecular structure of SMS1, including the transmembrane domains, should be clarified by further detailed analysis.

It was recently proposed by Luberto *et al.* (40) that the *Pseudomonas PlcH* gene product, which is a secreted protein, is a putative SM synthase. The SMS1 peptide was suggested to be an integral membrane protein and did not show any significant homology with the *PlcH* product.

The SMS1 cDNA Is Responsible for Sphingomyelin Synthase in Mammalian Cells—Huitema *et al.* (24) demonstrated the SM synthase activity in the yeast cells expressing SMS1 cDNA. Here, we demonstrated that the loss of SM synthesis in the SM-defective mammalian cells was complemented with SMS1 cDNA. WR19L/Fas-SM(−) cells transfected with SMS1 cDNA, named WR19L/Fas-SMS1 (Fig. 2*C*), restore the resistance against MβCD-induced cell death (Fig. 2*D*). Radiolabeling of cellular lipids with [^{14}C]serine revealed that [^{14}C]SM synthesis was also restored in WR19L/Fas-SMS1 cells (Fig. 3*A*), and whole cell lysate from WR19L/Fas-SMS1 cells generated C6-NBD-SM in the presence of C6-NBD-ceramide and PC (Fig. 3*B*). These results strongly suggest that the SMS1 cDNA is indispensable for SM synthase activity in mammalian cells. Furthermore, SM synthase activity in WR19L/Fas-SMS1 cells was detected in the presence of [^{14}C]PC but not [^{14}C]CDP-choline (Fig. 3*C*), suggesting that PC was a phosphocholine donor for SM synthesis by SMS1. These results indicate that the SMS1 protein possesses the characteristics consistent with those of SM synthase reported elsewhere previously (8).

The SMS1 cDNA Is Essential for Growth in Mammalian Cells—In contrast to the role of ceramide in cell death, the biological implications of SM are still ambiguous. The WR19L/Fas-SMS1 cells were sensitive to lysenin-induced cell death (Fig. 4*A*), suggesting that overexpression of SMS1 cDNA increases SM at the surface of plasma membrane. In the serum-free condition, the WR19L/Fas-SM(−) cells did not grow well, whereas the WR19L/Fas-SMS1 cells showed normal cell growth as well as the WR19L/Fas-SM(+) cells. The supplement with exogenous SM also restored cell growth of WR19L/Fas-SM(−) cells, although the growth rate was slightly reduced (Fig. 4*B*). The viable cell number of WR19L/Fas-SM(−) cells after 48 h from supplement with SM (4.4×10^5/ml) seemed to be similar to that of WR19L/Fas-SMS1 cells after 24 h (4.3×10^5/ml; data not shown), suggesting that stimulation for cell growth may be delayed due to the uptake of SM by WR19L/Fas-SM(−) cells. These observations suggest that SM synthesis through SM synthase is essential for cell growth. Huitema *et al.* (24) suggested that SMS2 is localized at the plasma membrane and may play a role in signal transduction. Here, we demonstrated that the cell growth was closely related with the accumulation of SM at the plasma membrane caused by SMS1, suggesting that SMS1 may be involved in signal transduction for cell growth as well as SMS2. In contrast to our observation, it has been reported that the variant melanoma cells deficient in glucosylceramide synthase showed no significant difference of cell growth as compared with the original cells (41), although glucosylceramide is an essential lipid for the diversity of glycosphingolipids. One possible explanation for the difference between SM and glucosylceramide is the significant involvement of SM in the microdomains responsible for various cell signaling events.

SM synthase regulates the levels of pro-apoptotic ceramide and anti-apoptotic DAG in an opposite manner and balances the levels of phospholipid PC and sphingolipid SM (9). SM synthase is closely regulated by the levels of ceramide and DAG, as well as extracellular stresses (15, 18, 31, 42). SM synthase is suggested to localize not only in the plasma membrane (37) and Golgi apparatus (43) but also in the endoplasmic reticulum (38) and nucleus (17, 44). We recently reported that, in Fas-induced Jurkat T cell apoptosis, ceramide increased through inhibition of SM synthase in the nucleus (17). The relationship between the intracellular localization and the regulation of SM synthase activity and the regulatory mechanism for the levels of lipid mediators in cell growth and death through SM synthase should be clarified by detailed analysis of the *SMS* genes.

Acknowledgments—We appreciate Dr. K. Hanada (National Institute of Infectious Diseases) for a useful support in terms of retroviral transfection and MβCD screening methods and Drs. Y. Hirabayashi (RIKEN) and Y. Igarashi (Hokkaido University) for careful discussions. We also appreciate Drs. A. Takaori and M. Kobayashi (Kyoto University) for a technical advice for retroviral transfection.

REFERENCES

1. English, D. (1996) *Cell. Signal.* **8**, 341–347
2. Majerus, P. W. (1992) *Annu. Rev. Biochem.* **61**, 225–250
3. Pettus, B. J., Chalfant, C. E., and Hannun, Y. A. (2002) *Biochim. Biophys. Acta* **1585**, 114–125
4. Okazaki, T., Kondo, T., Kitano, T., and Tashima, M. (1998) *Cell. Signal.* **10**, 685–692
5. Hannun, Y. A. (1994) *J. Biol. Chem.* **269**, 3125–3128
6. Moschetta, A., Portincasa, P., van Erpecum, K. J., Debellis, L., Vanberge-Henegouwen, G. P., and Palasciano, G. (2003) *Dig. Dis. Sci.* **48**, 1094–1101
7. Dillehay, D. L., Webb, S. K., Schmelz, E. M., and Merrill, A. H., Jr. (1994) *J. Nutr.* **124**, 615–620
8. Voelker, D. R., and Kennedy, E. P. (1982) *Biochemistry* **21**, 2753–2759
9. Hampton, R. Y., and Morand, O. H. (1989) *Science* **246**, 1050
10. Pagano, R. E. (1988) *Trends Biochem. Sci.* **13**, 202–205
11. Moscat, J., Cornet, M. E., Diaz-Meco, M. T., Larrodera, P., Lopez-Alanon, D., and Lopez-Barahona, M. (1989) *Biochem. Soc. Trans.* **17**, 988–991
12. Lucas, L., del Peso, L., Rodriguez, P., Penalva, V., and Lacal, J. C. (2000) *Oncogene* **19**, 431–437
13. Hannun, Y. A., and Bell, R. M. (1989) *Science* **243**, 500–507
14. Miro-Obradors, M. J., Osada, J., Aylagas, H., Sanchez-Vegazo, I., and Palacios-Alaiz, E. (1993) *Carcinogenesis* **14**, 941–946
15. Riboni, L., Tettamanti, G., and Viani, P. (2002) *Cerebellum* **1**, 129–135
16. Luberto, C., and Hannun, Y. A. (1998) *J. Biol. Chem.* **273**, 14550–14559
17. Watanabe, M., Kitano, T., Kondo, T., Yabu, T., Taguchi, Y., Tashima, M., Umehara, H., Domae, N., Uchiyama, T., and Okazaki, T. (2004) *Cancer Res.* **64**, 1–8
18. Itoh, M., Kitano, T., Watanabe, M., Kondo, T., Yabu, T., Taguchi, Y., Iwai, K., Tashima, M., Uchiyama, T., and Okazaki, T. (2003) *Clin. Cancer Res.* **9**,

415–423
19. Okazaki, T., Bell, R. M., and Hannun, Y. A. (1989) *J. Biol. Chem.* **264,** 19076–19080
20. Chatterjee, S. (1999) *Chem. Phys. Lipids* **102,** 79–96
21. Cremesti, A. E., Goni, F. M., and Kolesnick, R. (2002) *FEBS Lett.* **531,** 47–53
22. Hanada, K., Hara, T., Fukasawa, M., Yamaji, A., Umeda, M., and Nishijima, M. (1998) *J. Biol. Chem.* **273,** 33787–33794
23. Shakor, A. B., Czurylo, E. A., and Sobota, A. (2003) *FEBS Lett.* **542,** 1–6
24. Huitema, K., van den Dikkenberg, J., Brouwers, J. F. H. M., and Holthuis, J. C. M. (2004) *EMBO J.* **23,** 33–44
25. Yamaji-Hasegawa, A., Makino, A., Baba, T., Senoh, Y., Kimura-Suda, H., Sato, S. B., Terada, N., Ohno, S., Kiyokawa, E., Umeda, M., and Kobayashi, T. (2003) *J. Biol. Chem.* **278,** 22762–22770
26. Hanada, K., Kumagai, K., Yasuda, S., Miura, Y., Kawano, M., Fukasawa, M., and Nishijima, M. (2003) *Nature* **426,** 803–809
27. Yamaji, A., Sekizawa, Y., Emoto, K., Sakuraba, H., Inoue, K., Kobayashi, H., and Umeda, M. (1998) *J. Biol. Chem.* **273,** 5300–5306
28. Slotte, J. P. (1999) *Chem. Phys. Lipids* **102,** 13–27
29. Ostermeyer, A. G., Beckrich, B. T., Ivarson, K. A., Grove, K. E., and Brown, D. A. (1999) *J. Biol. Chem.* **274,** 34459–34466
30. Fukasawa, M., Nishijima, M., Itabe, H., Takano, T., and Hanada, K. (2000) *J. Biol. Chem.* **275,** 34028–34034
31. Fukasawa, M., Nishijima, M., and Hanada, K. (1999) *J. Cell Biol.* **144,** 673–685
32. Altschul, S. F., Gish, W., Miller, W., Myers, E. W., and Lipman, D. J. (1990) *J. Mol. Biol.* **215,** 403–410
33. Hirokawa, T., Boon-Chieng, S., and Mitaku, S. (1998) *Bioinformatics (Oxf.)* **14,** 378–379
34. Bork, P., and Koonin, E. V. (1998) *Nat. Genet.* **18,** 313–318
35. Barrera, F. N., Poveda, J. A., Gonzalez-Ros, J. M., and Neira, J. L. (2003) *J. Biol. Chem.* **278,** 46878–46885
36. Schultz, J., Ponting, C. P., Hofmann, K., and Bork, P. (1997) *Protein Sci.* **6,** 249–253
37. Futerman, A. H., Stieger, B., Hubbard, A. L., and Pagano, R. E. (1990) *J. Biol. Chem.* **265,** 8650–8657
38. van Helvoort, A., Stoorvogel, W., van Meer, G., and Burger, N. J. (1997) *J. Cell Sci.* **110,** 781–788
39. Elmendorf, H. G., and Haldar, K. (1994) *J. Cell Biol.* **124,** 449–462
40. Luberto, C., Stonehouse, M. J., Collins, E. A., Marchesini, N., El-Bawab, S., Vasil, A. I., Vasil, M. L., and Hannun, Y. A. (2003) *J. Biol. Chem.* **278,** 32733–32743
41. Ichikawa, S., Nakajo, N., Sakiyama, H., and Hirabayashi, Y. (1994) *Proc. Natl. Acad. Sci. U. S. A.* **91,** 2703–2707
42. Hanada, K., Horii, M., and Akamatsu, Y. (1991) *Biochim. Biophys. Acta* **1086,** 151–156
43. Allan, D., and Obradors, M. J. (1999) *Biochim. Biophys. Acta* **1450,** 277–287
44. Albi, E., and Magni, M. V. (1999) *FEBS Lett.* **460,** 369–372
45. Kyte, J., and Doolittle, R. F. (1982) *J. Mol. Biol.* **157,** 105–132

Peyer's Patch Dendritic Cells Capturing Oral Antigen Interact with Antigen-Specific T Cells and Induce Gut-Homing $CD4^+CD25^+$ Regulatory T Cells in Peyer's Patches

KATSUYA NAGATANI, KAYO SAGAWA, YOSHINORI KOMAGATA, AND KAZUHIKO YAMAMOTO

Department of Allergy and Rheumatology, Graduate School of Medicine, University of Tokyo, Tokyo, Japan

ABSTRACT: **Antigen-specific naive T cells accumulated in Peyer's patches only after the feeding of antigen. DCs that captured oral antigen interacted with these T cells in the IFR of PP. Some of these T cells acquired a similar phenotype to $CD4^+$ $CD25^+$ regulatory T cells and $CCR9^+$ gut-homing T cells.**

KEYWORDS: **Peyer's patch; dendritic cell; chemokine receptor; regulatory T cell**

INTRODUCTION

It is thought that antigen-specific regulatory T cells are generated in the gut-associated lymphoid tissue (GALT), including Peyer's patches (PPs), after antigen is orally administered. However, the importance of dendritic cells (DCs) in the generation of regulatory T cells, and the kind of regulatory T cells generated in PPs are still unclear. Here, we show that PP DCs capturing oral antigen interacted with antigen-specific T cells and induced gut-homing $CD4^+CD25^+$ regulatory T cells in PPs.

MATERIALS AND METHODS

We transferred naive T cells of ovalbumin (OVA)-TCR transgenic mice (DO11.10) into BALB/c mice, which were then fed FITC-conjugated OVA (FITC-OVA) (30 mg/mouse) 24 h later. Kinetics of oral antigen–loaded cells and interaction between antigen-specific T cells and antigen-loaded DCs in PPs after the feeding of OVA (or FITC-OVA) were checked by immunofluorescence staining.

Address for correspondence: Yoshinori Komagata, Department of Allergy and Rheumatology, Graduate School of Medicine, University of Tokyo, 7-3-1 Hongo, Bunkyo-ku, Tokyo 113-8655, Japan. Voice: +81-3-3815-5411, ext. 37263; fax: +81-3-3815-5954.
komagata-tky@umin.ac.jp

Ann. N.Y. Acad. Sci. 1029: 366–370 (2004).
doi: 10.1196/annals.1309.020

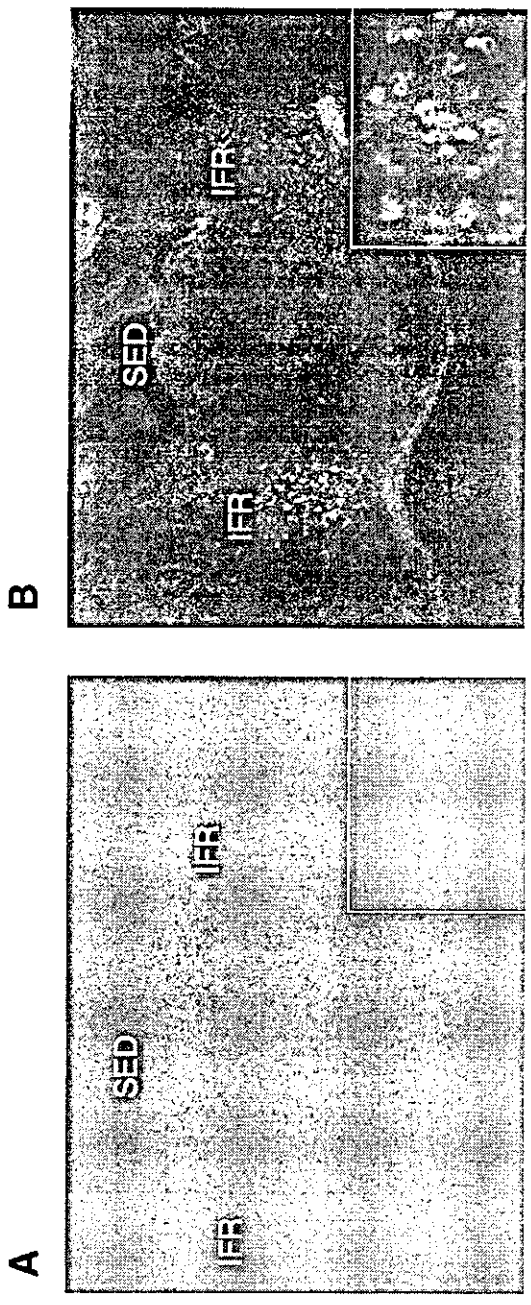

FIGURE 1. OVA-specific T cells accumulated in IFR of Peyer's patch by OVA feeding. We transferred OVA-specific T cells of DO11.10 mice into naive BALB/c mice, then fed 30 mg OVA to these mice. We collected Peyer's patches 24 h after the transfer and stained with FITC anti-KJ1.26 antibody. (A) Peyer's patch of nonfed mouse. OVA-specific T cells are not detected (inset magnified ×200). (B) Peyer's patch of OVA-fed mouse. OVA-specific T cells accumulated in IFR (inset magnified ×200).

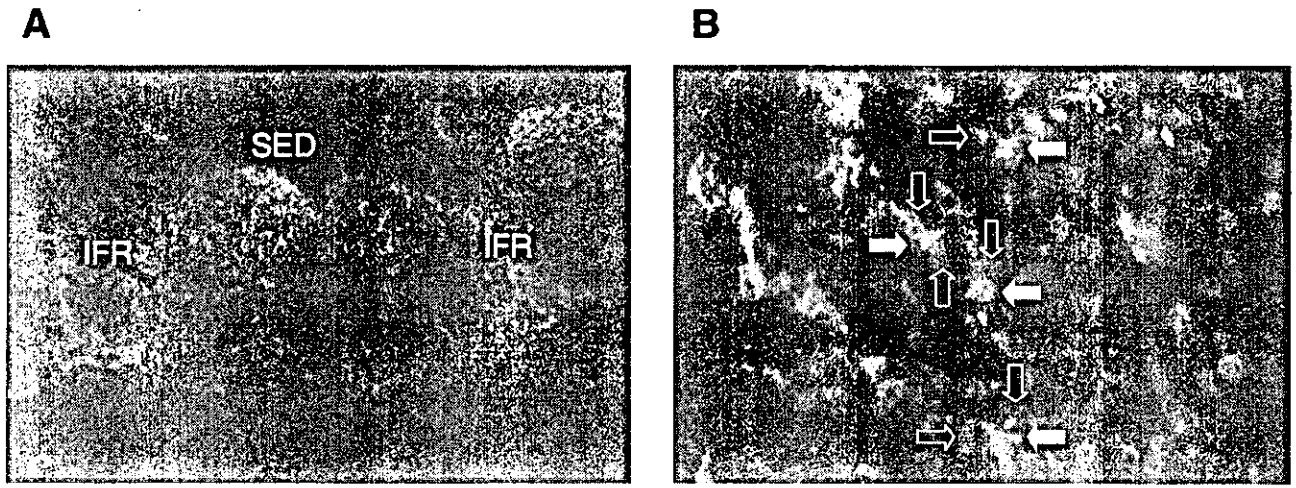

FIGURE 2. FITC-OVA–loaded DCs interact with OVA-specific T cells in IFR of Peyer's patches. (**A**) We transferred OVA-specific T cells of DO11.10 mice into naive BALB/c mice, then fed 30 mg of FITC-conjugated OVA (FITC-OVA) to these mice. We collected Peyer's patches 24 h after the transfer, and stained with FITC anti-KJ1.26 antibody and PE anti-CD11c antibody. (IFR, interfollicular region; SED, subepithelial dome; magnified ×40). (**B**) FITC-OVA–loaded DCs (*closed arrows*) contact OVA-specific T cells (*open arrows*) in IFR after FITC-OVA feeding (magnified ×400).

To examine the phenotype of OVA-specific T cells accumulated in PPs after OVA feeding, we purified KJ1.26 positive T cells from PPs by magnetic beads (MACS, Miltenyi Biotec, Bergisch Gladbach, Germany) and checked relative gene expression by real-time RT-PCR (iCycler iQ; Bio-Rad, CA).

RESULTS

FITC-positive cells appeared in the subepithelial dome (SED) of PPs as early as three hours after the feeding of FITC-OVA. Double staining with PE anti-CD11c antibody showed that FITC-positive cells in SEDs were CD11c-positive DCs (data not shown). Twenty-four hours after the feeding of FITC-OVA, DCs capturing FITC-OVA migrated from the SED to the interfollicular region (IFR) and interacted with OVA-specific T cells accumulated in the IFR of PPs (FIG. 1B and FIG. 2). In contrast, OVA-specific T cells were not detected in IFRs in nonfed mice (FIG. 1A).

We investigated the gene expression levels of chemokine receptors such as CCR4, CCR7, CCR8, CCR9, and CXCR3 in OVA-specific T cells by quantitative

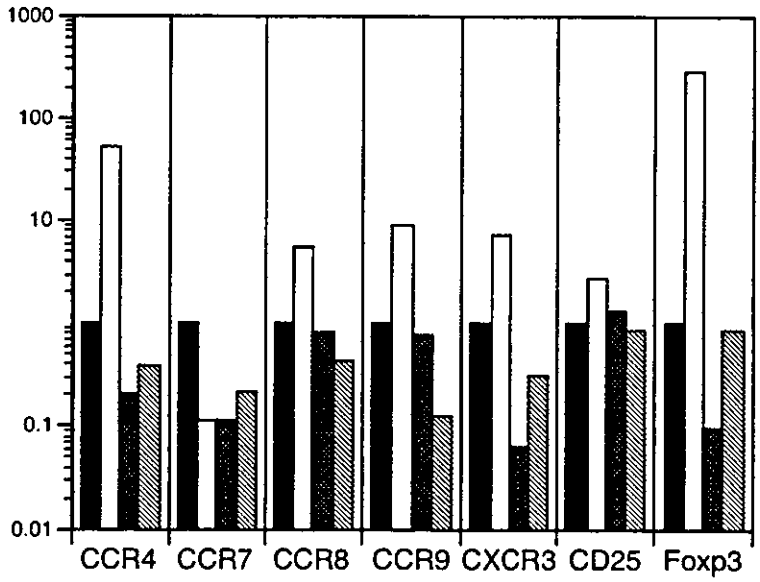

FIGURE 3. Gene expression in OVA-specific T cells accumulating in Peyer's patches after OVA feeding. We transferred OVA-specific T cells of DO11.10 mice into naive BALB/c mice, followed by feeding of 30 mg OVA. Twenty-four hours after the transfer, KJ1.26-positive OVA-specific T cells were purified from Peyer's patches, and total RNA was extracted. We checked relative gene expression of OVA-specific T cells accumulated in Peyer's patch by quantitative real time RT-PCR (*open box*). As controls, KJ1.26-positive T cells from spleens of OVA-fed (*black box with white dots*), nonfed mice (*striped box*), and KJ1.26-positive T cells before transfer (*black box*) were also checked.

real-time PCR. Gene expression of CCR4, CCR8, CCR9, and CXCR3 was substantially higher in OVA-specific T cells accumulated in PPs after OVA feeding (FIG. 3).

It has been reported that CCR4 and CCR8 are expressed on $CD4^+CD25^+$ regulatory T cells.[1] Therefore, we next checked the gene expression of Foxp3, which is a $CD4^+CD25^+$ regulatory T cell–specific transcription factor,[2] in OVA-specific T cells. Surprisingly, the Foxp3 gene level in OVA-specific T cells accumulated in PPs after OVA feeding was 294-fold more abundant than in OVA-specific T cells before the transfer. Expression of CCR7, which is regarded as a marker of naive T cells, in the OVA-specific T cells before the transfer, was relatively high (FIG. 3).

DISCUSSION

Recent studies have shown that CCR4, CCR8, and CXCR3 are expressed on $CD4^+CD25^+$ regulatory T cells and that Foxp3 is exclusively expressed in these T cells.[1,2] In addition, CCR9 has been reported to be expressed by gut-homing T cells.[3] These results suggest that DCs that capture oral antigens in the SED migrate into the IFR and interact with antigen-specific T cells, and that some antigen-specific T cells acquire a similar phenotype to $CCR9^+$ gut-homing T cells and $CD4^+CD25^+$ regulatory T cells.

REFERENCES

1. IELLEM, A., M. MARIANI, R. LANG, *et al.* 2001. Unique chemotactic response profile and specific expression of chemokine receptors CCR4 and CCR8 by $CD4^+CD25^+$ regulatory T cells. J. Exp. Med. **194:** 847–854.
2. HORI, S., T. NOMURA & S. SAKAGUCHI. 2003. Control of regulatory T cell development by the transcription factor Foxp3. Science **299:** 1057–1061.
3. ZABEL, B.A., W.W. AGACE, J.J. CAMPBELL, *et al.* 1999. Human G protein–coupled receptor GPR-9-6/CC chemokine receptor 9 is selectively expressed on intestinal homing T lymphocytes, mucosal lymphocytes, and thymocytes and is required for thymus-expressed chemokine–mediated chemotaxis. J. Exp. Med. **190:** 1241–1256.

 Related Commentary, page 471

Distinct contribution of IL-6, TNF-α, IL-1, and IL-10 to T cell–mediated spontaneous autoimmune arthritis in mice

Hiroshi Hata,[1,2] Noriko Sakaguchi,[1,3] Hiroyuki Yoshitomi,[1,2] Yoichiroh Iwakura,[4] Kenji Sekikawa,[5] Yoshiaki Azuma,[6] Chieko Kanai,[7] Eiko Moriizumi,[7] Takashi Nomura,[1] Takashi Nakamura,[2] and Shimon Sakaguchi[1,3,8]

[1]Department of Experimental Pathology, Institute for Frontier Medical Sciences, Kyoto University, Kyoto, Japan. [2]Department of Orthopedic Surgery, Faculty of Medicine, Kyoto University, Kyoto, Japan. [3]Laboratory for Immunopathology, RIKEN Research Center for Allergy and Immunology, Yokohama, Japan. [4]Institute of Medical Sciences, Tokyo University, Tokyo, Japan. [5]Department of Molecular Biology and Immunology, National Institute of Agrobiological Sciences, Tsukuba, Ibaraki, Japan. [6]Teijin Institute for Biomedical Research, Teijin Pharma Ltd., Tokyo, Japan. [7]Tokyo Metropolitan Institute of Gerontology, Tokyo, Japan. [8]Core Research for Evolutional Science and Technology (CREST), Japan Science and Technology Agency, Kawaguchi, Japan.

Cytokines play key roles in spontaneous CD4⁺ T cell–mediated chronic autoimmune arthritis in SKG mice, a new model of rheumatoid arthritis. Genetic deficiency in IL-6 completely suppressed the development of arthritis in SKG mice, irrespective of the persistence of circulating rheumatoid factor. Either IL-1 or TNF-α deficiency retarded the onset of arthritis and substantially reduced its incidence and severity. IL-10 deficiency, on the other hand, exacerbated disease, whereas IL-4 or IFN-γ deficiency did not alter the disease course. Synovial fluid of arthritic SKG mice contained high amounts of IL-6, TNF-α, and IL-1, in accord with active transcription of these cytokine genes in the afflicted joints. Notably, immunohistochemistry revealed that distinct subsets of synovial cells produced different cytokines in the inflamed synovium: the superficial synovial lining cells mainly produced IL-1 and TNF-α, whereas scattered subsynovial cells produced IL-6. Thus, IL-6, IL-1, TNF-α, and IL-10 play distinct roles in the development of SKG arthritis; arthritogenic CD4⁺ T cells are not required to skew to either Th1 or Th2; and the appearance of rheumatoid factor is independent of joint inflammation. The results also indicate that targeting not only each cytokine but also each cell population secreting distinct cytokines could be an effective treatment of rheumatoid arthritis.

Introduction

Rheumatoid arthritis (RA) is a chronic systemic inflammatory disease of unknown etiology that primarily affects the synovial membranes of multiple joints (1). A cardinal feature of joint inflammation in RA is proliferative inflammation of synovial cells, i.e., synovitis, which results in the destruction of the adjacent cartilage and bone. Although CD4⁺ T cells are currently assumed to be the prime mediators of synovitis, it remains obscure how arthritogenic CD4⁺ T cells activate synovial cells to proliferate or, upon activation, how the autonomous proliferation of synovial cells is maintained, leading to the destruction of the joint (1). It has been well documented that cytokines play indispensable roles in these processes (2). TNF-α and IL-6, for example, contribute to joint inflammation in RA, as illustrated by the effects of neutralizing TNF-α or blocking IL-6 receptor to ameliorate RA (3, 4). IFN-γ, IL-4, and IL-10 formed by Th1 or Th2 CD4⁺ T cells may also participate in synovitis, as observed in other autoimmune diseases (1, 2). The way in which these cytokines contribute to the development of arthritides including RA, however, is a subject of controversy, as cytokines exert different effects in different models of arthritis. For example, IL-6 deficiency variously results in exacerbation of, amelioration of, or no effects on arthritis, depending on the particular model (5–9). Neutralization of TNF-α has different effects in collagen-induced arthritis (CIA) and streptococcal cell wall–induced arthritis (10). IFN-γ may not only mediate Th1 responses in arthritis but also suppress the destruction of cartilage and bone by inhibiting the generation of osteoclasts (11). Furthermore, it is unclear how relevant the available arthritis models are to human RA. For example, CIA, one of the most widely used models of RA, is not accompanied by the appearance of rheumatoid factor (RF), which is present in about 70% of RA patients (1). In this report, we have analyzed the contribution of pro- and anti-inflammatory cytokines to the spontaneous development and chronic progression of CD4⁺ T cell–mediated autoimmune arthritis in a newly established mouse model of RA.

SKG mice spontaneously develop T cell–mediated chronic autoimmune arthritis as a consequence of a mutation of the gene encoding an Src homology 2 (SH2) domain of ζ-associated protein of 70 kDa (ZAP-70), a key signal transduction molecule in T cells (12). This mutation impairs positive and negative selection of T cells in the thymus, leading to thymic production of arthritogenic T cells. Clinically, joint swelling begins in small joints of the digits, progressing in a symmetrical fashion to larger joints including wrists and ankles. Histologically, the swollen joints show severe synovitis with formation of pannus invading and eroding adjacent cartilage and subchondral bone. SKG mice develop extra-articular lesions, such as interstitial pneumonitis, vasculitides, and subcuta-

Nonstandard abbreviations used: ζ-associated protein of 70 kDa (ZAP-70); collagen-induced arthritis (CIA); rheumatoid arthritis (RA); rheumatoid factor (RF); Src homology 2 (SH2).

Conflict of interest: The authors have declared that no conflict of interest exists.

Citation for this article: *J. Clin. Invest.* 114:582–588 (2004). doi:10.1172/JCI200421795.

neous necrobiotic nodules not unlike rheumatoid nodules in RA. Serologically, they develop high titers of RF and autoantibodies specific for type II collagen. Furthermore, $CD4^+$ T cells can adoptively transfer arthritis in SKG mice, which have a BALB/c genetic background, to T cell–deficient BALB/c nude or T cell/B cell–deficient SCID mice, which indicates that the disease is a T cell–mediated autoimmune disease. In addition to the causative gene, the polymorphism of the *MHC* gene also contributes to the occurrence of SKG arthritis depending on environmental conditions. Thus, this spontaneous autoimmune arthritis in mice resembles human RA in clinical and histological characteristics of articular and extra-articular lesions, in serological characteristics, and in the key role of $CD4^+$ T cells in initiating arthritis (12).

In contrast to other organ-specific autoimmune diseases in which self-reactive T cells destroy the target cells (e.g., insulin-secreting β cells in type 1 diabetes mellitus), a key feature of SKG autoimmune arthritis, and human RA for that matter, is that T cells do not destroy but stimulate synoviocytes to proliferate and invade the surrounding cartilage and bone. The selective development of arthritis in SKG mice, despite their general alteration in the T cell repertoire, could be attributed at least in part to a high sensitivity of synoviocytes to immunological stimuli, including T cell self-reactivity, due to their immunologically unique features. The synoviocytes are, for example, intrinsically capable of producing proinflammatory cytokines and matrix metalloproteinases; are composed of type A macrophage-like and type B fibroblast-like synoviocytes, both of which are highly sensitive to various immunological stimuli including cytokines; and are devoid of basement membrane and tight junctions, allowing their easy invasion to the surrounding tissue (1). We have therefore analyzed in this report how the synoviocytes stimulated by arthritogenic $CD4^+$ T cells mediate arthritis in SKG mice and how those cytokines produced by the stimulated synoviocytes or arthritogenic $CD4^+$ T cells contribute to the development and progression of arthritis.

Results

Clinical and histological features of SKG arthritis. In SKG mice, joint swelling began to develop in a few digits around 2 months of age, progressing to other digits and to larger joints (wrists and ankles) in a symmetrical fashion (Supplemental Figure 1; supplemental material available at http://www.jci.org/cgi/content/full/114/4/582/DC1). Histology of swollen joints showed vigorous proliferation of synovial cells, resulting in pannus formation and infiltration of mononuclear cells and neutrophils to the subsynovial region (Supplemental Figure 2). Pannus-destroyed cartilage and bone showed the appearance of multinuclear osteoclasts at the interface between invading synovial tissue and the adjacent cartilage and subchondral bone. Synoviocytes that formed a few layers of superficial lining of pannus were characteristically tall and plump and bore a large cytoplasm, as shown by H&E staining. Electron microscopy revealed that the majority of these superficial lining cells were type B fibroblast-like synoviocytes with occasional type A macrophage-like synoviocytes (Supplemental Figure 3). It also showed infiltration of lymphocytes and neutrophils to the sublining region and some synoviocytes apparently in apoptosis, as has been observed in human RA (13). In 8-month-old SKG mice, microcomputerized tomography revealed erosion of the cartilage and subchondral bone in knee joints (Supplemental Figure 4). Thus, SKG mice develop severe proliferative synovitis accompanying destruction of cartilage and subchondral bone of digits, wrists, ankles, and knees, as do humans with RA (1).

Immunohistochemistry of SKG synovitis. Immunohistochemical staining of synovial tissues of 4-month-old SKG mice with various antibodies revealed the following. A number of $CD4^+$ T cells, but few $CD8^+$ T cells, infiltrated the sublining tissue, where B cells also formed aggregates (Figure 1, A–C). Granulocytes (Figure 1D) and macrophages (Figure 1E) were abundant in the joint cavity and also subsynovial region. The distribution of macrophages corresponded to that of class II MHC–expressing cells (Figure 1F). Many cells expressing CD49d (also known as very late antigen 4; VLA-4) infiltrated the subsynovia (Figure 1G), and its ligand VCAM-1 was expressed in vascular endothelial cells and interstitial cells (Figure 1H), which indicates recruitment of lymphocytes to the inflamed synovial tissue (Figure 1I) (14). Toluidine blue staining revealed few mast cells in the inflamed tissue (data not shown).

Cytokine production in arthritic joints. Ankle joints of the majority of 24-week-old SKG mice with severe joint swelling exhibited high-level expression of IL-1β and IL-6 mRNA, as assessed by real-time RT-PCR; half of the mice also actively transcribed TNF-α mRNA (Figure 2A). In contrast, 8-week-old SKG mice without apparent joint swelling showed no IL-6 transcription and only a slight expression of IL-1β, although TNF-α mRNA was detected in some young SKG mice. IL-2, IL-4, IL-10, and IFN-γ mRNA messages were not detected even in 24-week-old SKG mice (data not shown).

The joint fluid taken from swollen ankle joints of 32-week-old SKG mice contained high amounts of IL-1β, IL-6, and TNF-α (Figure 2B). Serum levels of these cytokines were below detectable levels by ELISA in the majority of mice, although 20% of them bore low but significant amounts of IL-6 in their sera (data not shown).

Immunohistochemical staining of inflamed synovial tissue of SKG mice revealed distinct staining patterns of TNF-α and IL-1β versus IL-6. Cells expressing IL-1β and TNF-α were detected almost exclusively in one or two layers of hypertrophic superficial lining cells facing the joint cavity (Figure 2, C and D). In contrast, cells expressing IL-6 were smaller than the superficial

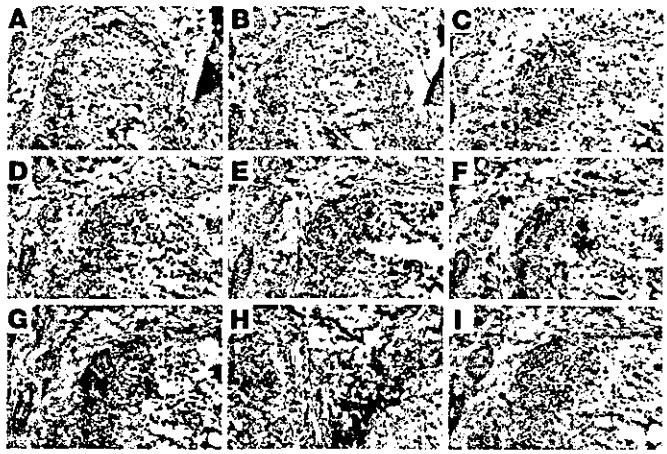

Figure 1
Immunohistology of synovitis. Serial sections of a finger joint of a 5-month-old SKG mouse were stained for CD4 (**A**), CD8 (**B**), B220 (**C**), Gr-1 (**D**), CD11b (**E**), I-A/I-E (**F**), CD49d (**G**), or VCAM-1 (**H**) with staining control (**I**). Arrow indicates vasculature. Original magnification, ×20.

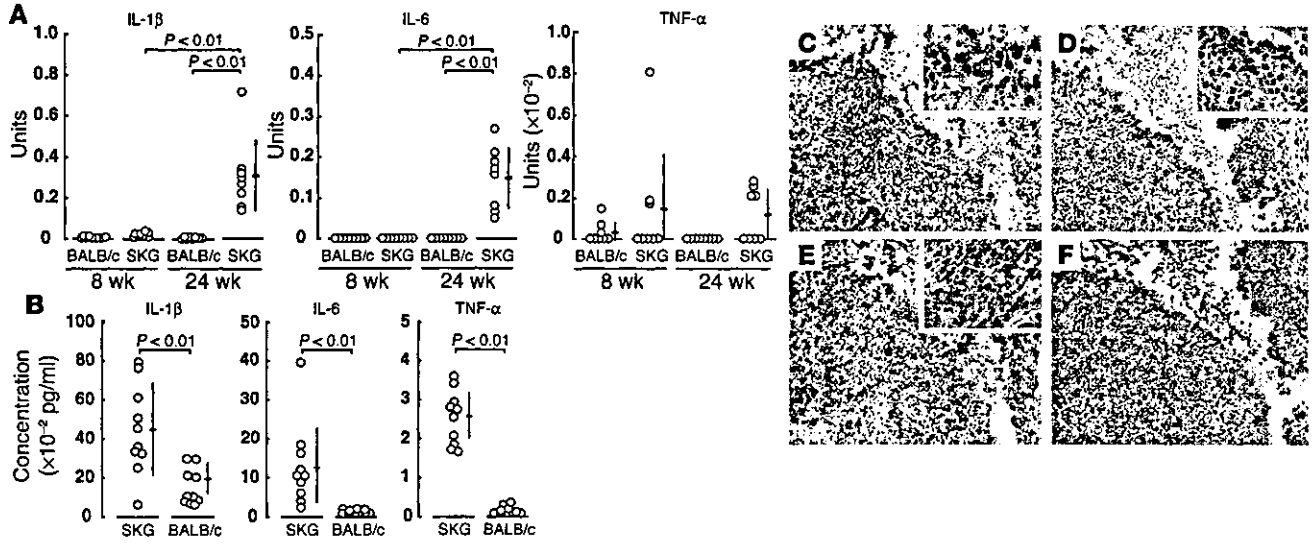

Figure 2

Expression of cytokines at mRNA and protein levels. (**A**) Quantitative RT-PCR for indicated genes was performed with ankle joints from 8- or 24-week-old SKG or BALB/c mice. Bars show the means ± SD. See Methods for the definition of units. (**B**) Concentrations of indicated cytokines, assessed by ELISA, in the joint fluid of 32-week-old SKG and BALB/c mice (n = 10 each). Bars show the means ± SD. (**C–F**) Immunohistochemical staining of the synovial tissue of a finger joint of a 4-month-old SKG mouse for IL-1β (**C**), TNF-α (**D**), or IL-6 (**E**), with staining control (**F**) (original magnification, ×40). Insets show higher magnifications of a part of synovium.

lining cells and scattered in the sublining region (Figure 2E). The localization of IL-6–expressing cells correlated with that of MAC-1$^+$, I-A/I-E$^+$ macrophages or CD4$^+$ cells (Figure 1).

These results collectively indicate that the inflamed synovial tissue of SKG mice actively produces IL-1β, TNF-α and IL-6; the cells forming TNF-α and IL-1β are apparently the same and constitute the superficial lining layer; and the cells mainly forming IL-6 are apparently different from those forming IL-1β and TNF-α and localize differently.

Effect of deficiency in particular cytokines on the development and progression of SKG arthritis. To determine the roles of proinflammatory cytokines IL-1α, IL-1β, TNF-α, and IL-6 in the development of SKG arthritis, homozygously cytokine gene-deficient (–/–), heterozygously cytokine gene-deficient (+/–), or cytokine gene-intact (+/+) female SKG mice were prepared and maintained in our conventional animal facility, where the majority of cytokine gene-intact female SKG mice began to exhibit joint swelling at 11 to 12 weeks of age (Figure 3A). Severity of arthritis in these mice varied from swelling of some joints of the digits to marked swelling of large joints (the average score was 3.6 ± 1.5; see Methods for clinical assessment of arthritis) at 32 weeks of age. Histology of swollen joints of 32-week-old SKG mice revealed severe synovitis and destruction of cartilage and bone (Figure 3B). Notably, IL-6$^{-/-}$ SKG mice showed no joint swelling macroscopically, no histologically evident synovitis, and no destruction of cartilage and bone (Figure 3C). Some IL-1α/β$^{-/-}$ SKG mice started to develop arthritis around 15 weeks of age with a significantly lower incidence than IL-1α/β$^{+/+}$ SKG mice. Although the incidence in IL-1$^{-/-}$ mice was 60% at 32 weeks of age, severity was very low, with joint swelling restricted to only 1 or 2 joints of the digits. These swollen joints showed histologically evident synovitis but destruction of cartilage and bone was generally less severe than in cytokine-intact SKG mice (data not shown). These results were similar in the TNF-α$^{-/-}$ SKG mice: the onset was delayed, incidence lowered to 20% of controls, and severity substantially reduced to swelling of a single joint of a digit (see legend to Figure 3A for statistical analyses of the data).

Interstitial pneumonitis — which was observed in SKG mice older than 8 months (12) — among these cytokine-deficient mice was too mild in severity and low in incidence at 32 weeks of age for comparisons to be made (data not shown).

IFN-γ–deficient SKG mice developed arthritis with no statistically significant differences in severity and incidence from IFN-γ$^{+/-}$ or IFN-γ$^{+/+}$ mice during 24 weeks of observation, although IFN-γ$^{-/-}$ SKG mice displayed progressive weight loss and died earlier as compared with wild-type controls maintained under the same conditions (12). We did not observe significant difference in histology between IFN-γ$^{-/-}$ and IFN-γ$^{+/-}$ or IFN-γ$^{+/+}$ mice, although the IFN-γ$^{-/-}$ mice, when they became debilitated, generally showed lesser degrees of arthritis compared with the IFN-γ$^{+/-}$ or IFN-γ$^{+/+}$ mice (data not shown). IL-4$^{-/-}$ SKG mice, on the other hand, survived well to 32 weeks of age; the time of onset, incidence and severity of arthritis were not significantly different among IL-4$^{-/-}$, IL-4$^{+/-}$, or IL-4$^{+/+}$ mice. Thus, IFN-γ and IL-4 are apparently dispensable for the development of SKG arthritis.

IL-10$^{-/-}$ SKG mice showed a consistently higher incidence of disease and mean arthritis score than IL-10$^{+/-}$ or IL-10$^{+/+}$ SKG mice, although the susceptibility to colitis of IL-10$^{-/-}$ mice restricted the period of observation to 24 weeks (15). Histological examination of IL-10$^{-/-}$ mice that had survived to this age showed severe synovitis accompanying joint destruction (Figure 3D). Thus, IL-10 is suppressive for the development of SKG arthritis.

In these experiments, SKG mice with heterozygous deficiency in IL-1, TNF-α, IL-6, or IL-10 showed incidences and severities of arthritis that were intermediate between those of homozygously cytokine-deficient and cytokine-intact mice. This result indicates that the disease-enhancing or -protective effects of the cytokines are dose dependent.

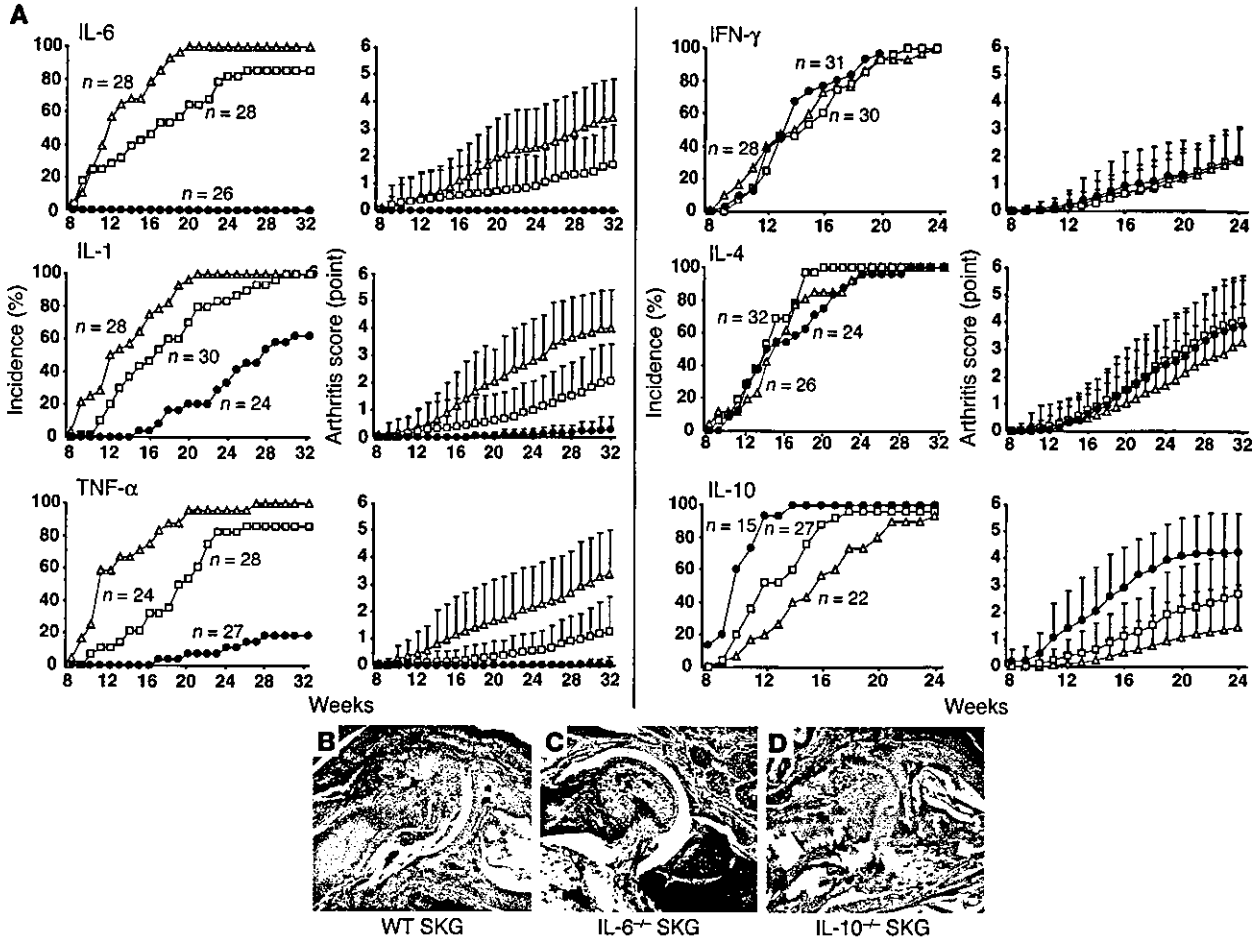

Figure 3

Development of arthritis in cytokine-deficient SKG mice. (**A**) Incidence and severity of arthritis in female SKG mice homozygously (–/–) (filled circles) or heterozygously (+/–) (open squares) deficient in indicated cytokines or cytokine-intact (+/+) (open triangles). Vertical bars represent the means ± SD of the whole group of mice. Arthritis scores are significantly different ($P < 0.01$) between IL-6$^{+/+}$ and IL-6$^{+/-}$ mice at 19–32 weeks; between IL-6$^{+/-}$ and IL-6$^{-/-}$ mice at 16–32 weeks; between IL-1$^{+/+}$ and IL-1$^{+/-}$ mice at 17–32 weeks; between IL-1$^{-/-}$ and IL-1$^{+/-}$ mice at 19–32 weeks; between TNF-α$^{+/+}$ and TNF-α$^{+/-}$ mice at 15–32 weeks; between TNF-α$^{-/-}$ and TNF-α$^{+/-}$ mice at 21–32 weeks; between IL-10$^{+/+}$ and IL-10$^{+/-}$ mice at 18–24 weeks; and between IL-10$^{-/-}$ and IL-10$^{+/-}$ mice at 12–24 weeks. (**B–D**) Histology of finger joints of a 32-week-old wild-type (**B**) or IL-6–deficient (**C**) or a 24-week-old IL-10–deficient SKG mouse (**D**) (original magnification, ×10).

RF and joint inflammation. The IL-6-, TNF-α-, or IL-1-deficient mice developed high titers of IgM-type RF even in the absence of joint inflammation (Figure 4A). This indicates that the development of IgM-RF is independent of joint inflammation. The result contrasted with the development of IgG anti-type II collagen autoantibody in arthritic mice but not in nonarthritic IL-6-deficient mice, which suggests the possible roles of anti-type II collagen antibody as an active mediator of joint inflammation or a product of joint destruction (Figure 4B).

Discussion

This study showed that proliferative synovitis with pannus formation and resultant joint destruction in SKG mice are immunopathologically similar to those observed in human RA and that, despite the pleiotropy, redundancy, and cross-regulation in cytokine functions, deficiency in either IL-6, IL-1, or TNF-α can inhibit the development and progression of SKG arthritis, which is apparently independent of the development of RF.

It is well documented in human RA and in animal models that IL-1, IL-6, and TNF-α synergistically mediate synovitis and destruction of cartilage and bone (1–3, 5, 6, 16–19), that IL-1 and TNF-α trigger the secretion of IL-6 by synovial cells (2), and that anti–TNF-α treatment can lower IL-6 formation (20, 21). It is still unclear, however, how the formation and action of these cytokines are controlled at molecular and cellular levels (22–24). Here we showed that IL-6 is apparently produced by subsynovial stromal cells (macrophages and DCs; Figure 1) and presumably some CD4$^+$ T cells, whereas IL-1 and TNF-α are mainly produced by superficial lining cells facing the joint cavity and producing matrix metalloproteinases as also shown in other arthritis models and RA (25–28). This difference in cellular sources between IL-6 and IL-1/TNF-α indicates that not only neutralization of these cytokines or blockade of their actions at a molecular level, but also reduction in the number of the stromal cells producing each cytokine or modifying their functions may ameliorate arthritis.

TNF-α deficiency inhibited arthritis effectively but not completely in SKG mice; i.e., the onset was delayed, incidence lowered

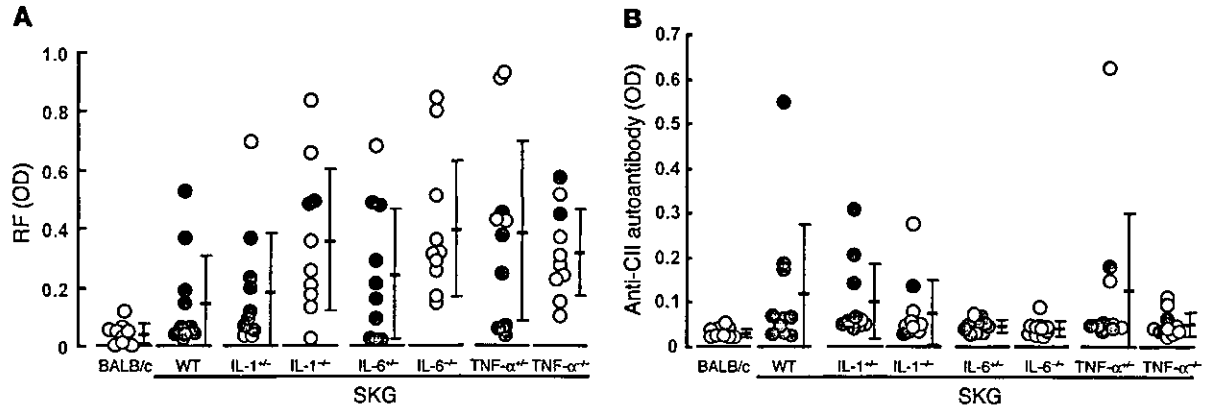

Figure 4

Autoantibodies in cytokine-deficient SKG mice. RF (**A**) or anti–type II collagen (anti-CII) autoantibody titers (**B**) in 32-week-old SKG mice homozygously or heterozygously deficient in indicated cytokines, with wild-type SKG mice and age-matched BALB/c mice as controls. Filled circles indicate mice with joint swelling (arthritis score ≥ 1.0); open circles indicate mice without joint swelling (arthritis score < 1.0). First 10 mice that had reached 32 weeks of age in each group shown in Figure 3 were analyzed.

to 20% of controls, and severity substantially reduced to swelling of a single joint of a digit. It can be argued that the MHC haplotype of TNF-α–deficient SKG mice could influence the development of arthritis, since TNF-α–deficient SKG mice bear an H-2b haplotype in contrast with SKG mice, which bear an H-2d haplotype. This is because the founder strain of TNF-α deficiency was of H-2b haplotype, and the TNF-α locus, which is closely linked with the MHC locus, was cosegregated with the MHC in establishing the congenic TNF-α–deficient SKG mice (29). We previously showed that the MHC haplotype of SKG mice can influence the incidence and severity of arthritis (e.g., H-2d haplotype confers susceptibility to arthritis in SKG mice [ref. 12]). It is unlikely, however, that the H-2b haplotype of TNF-α–deficient SKG mice alters the incidence and severity of arthritis, because SKG mice on BALB.B (H-2b) background showed an incidence and severity of arthritis similar to those of SKG mice (our unpublished data). Thus, TNF-α deficiency per se can inhibit the development of arthritis. On the other hand, the failure of TNF-α deficiency to completely inhibit arthritis suggests that proinflammatory cytokine pathways that spare TNF-α may also be operative in SKG arthritis. This substantial but incomplete inhibition of SKG arthritis by TNF-α deficiency may have a common basis with the clinical result that only about 30–40% of RA patients show dramatic responses to TNF inhibitors (30).

It is well documented in arthritis that pro- or anti-inflammatory cytokines facilitate or inhibit activation of various types of cells, including macrophages/monocytes, neutrophils, and T cells, which are involved in local inflammation (16). Another function of cytokines may be to alter the degree of T cell–mediated control of autoimmune T cells, thereby allowing arthritogenic T cells to chronically mediate arthritis. For example, IL-10 not only suppresses the formation of TNF-α and IL-6 by macrophages, synoviocytes, and T cells, as shown in other experimental models (31–33), but also may mediate or augment $CD25^+CD4^+$ T cell–mediated immunoregulation, as shown in other autoimmune/inflammatory diseases (34, 35). IL-10 deficiency may therefore attenuate the T cell–mediated suppression on arthritogenic T cells, thus contributing to the exacerbation of arthritis in SKG mice. Furthermore, in addition to its local and systemic proinflammatory effects (20, 36), IL-6 may render arthritogenic T cells refractory to the suppressive control exerted by naturally arising $CD25^+CD4^+$ regulatory T cells (37). $CD25^+CD4^+$ T cells, derived from normal BALB/c mice, indeed prevented SKG arthritis effectively when the animals were inoculated before onset of the disease, as observed in CIA (ref. 38 and our unpublished data). We are currently investigating whether IL-6 deficiency rectifies the susceptibility of arthritogenic T cells to the $CD25^+CD4^+$ T cell–mediated suppression and thereby contributes to inhibiting the development of SKG arthritis. Whether TNF-α or IL-1 can affect T cell–mediated immunoregulation by altering the functions of APCs or regulatory T cells also remains to be determined (39).

Although $CD4^+$ T cells play pivotal roles in SKG arthritis, they show impaired activation and proliferation upon T cell receptor stimulation because of a structurally altered ZAP-70 and resulting alteration in T cell signal transduction in SKG T cells (12). Despite this defect, SKG T cells are competent in secreting various cytokines, including IL-2, IL-4, IL-10, TNF-α, and IFN-γ, upon PMA/ionomycin stimulation, in a pattern of cytokine production and kinetics similar to that of BALB/c T cells (Supplemental Figure 5A). $CD4^+$ T cells from young SKG mice even produced slightly higher amounts of IFN-γ, IL-4, and IL-10 and smaller amounts of TNF-α than BALB/c $CD4^+$ T cells (Supplemental Figure 5B). Moreover, there was no significant alteration of the disease course in SKG mice with IFN-γ or IL-4 deficiency, which is in contrast with other models (40, 41). These findings taken together indicate that SKG $CD4^+$ T cells are not committed to Th1 or Th2 cells, or TNF-α production, due to the altered signal transduction through ZAP-70; skewing of $CD4^+$ arthritogenic T cells to either Th1 or Th2 is not absolutely required for the development and/or progression of arthritis; and cross-regulation, if any, by Th1 or Th2 cells is not significant in inhibiting arthritis in this model. It is possible that T cells in SKG mice trigger the activation and proliferation of synoviocytes in a cell-contact manner or via other cytokines (42). Notably, a large amount of mRNA for IL-17, which is secreted by activated T cells and able to stimulate synovial cells (43), can be detected in the joints of arthritic SKG mice (our unpublished data).

The disease in SKG mice is a chronic systemic inflammatory disease like human RA (1, 12). For example, SKG mice spontaneously develop RF as a systemic manifestation of the disease. An intriguing finding in cytokine-deficient SKG mice is that they developed high

titers of RF irrespective of whether arthritis was inhibited or not. For example, IL-6–deficient mice with no arthritis developed titers of RF equivalent to those of SKG mice. This cannot be attributed to hypergammaglobulinemia in SKG mice, because SKG mice without arthritis did not develop anti-DNA autoantibodies or anti-type II collagen autoantibodies, which may mediate joint inflammation or develop as a consequence of joint destruction (Figure 4) (12). Furthermore, transfer of thymocytes alone from SKG mice produced severe arthritis in SCID mice, which suggests that B cells may not be an absolute requirement for elicitation and progression of arthritis in this model (12). These results taken together indicate that RF is independent of joint inflammation per se in SKG mice. It is known, on the other hand, that RA patients with RF undergo a more aggressive and destructive course of arthritis (1). Considering that RF also develops in various other inflammatory diseases including microbial infections, it is likely that RF may not be a primary mediator of arthritis but may secondarily enhance joint inflammation, for example, by forming immune complexes that deposit in the joint (44, 45).

In conclusion, cytokines play essential roles in SKG arthritis in a manner similar to that in human RA. SKG mice can be instrumental for further studying the contribution of pro- and anti-inflammatory cytokines to the development and progression of RA, for elucidating how arthritogenic T cells stimulate synoviocytes to cause arthritis, and for devising effective treatment of the disease.

Methods

Mice. IL-1α/β–, TNF-α–, or IL-6–deficient mice (IL-1$^{-/-}$, TNF-α$^{-/-}$, and IL-6$^{-/-}$, respectively) were backcrossed to BALB/c mice more than 8 times (29). BALB/c IL-10–deficient (IL-10$^{-/-}$) mice were kindly provided by D. Rennick (DNAX Institute, Palo Alto, California, USA) (15). BALB/c IFN-γ$^{-/-}$ and IL-4$^{-/-}$ mice were purchased from The Jackson Laboratory (Bar Harbor, Maine, USA) (46, 47). These cytokine-deficient BALB/c mice were backcrossed three times to SKG mice, which have the BALB/c genetic background (12). Such *Skg*-homozygous but cytokine gene–heterozygous mice were intercrossed, and resulting female *Skg/Skg* littermates with homozygously or heterozygously cytokine-deficient or cytokine-intact female mice were used in the present study. All mice were maintained in our animal facility under conventional microbial conditions. All experiments were conducted according to the institutional guidelines for animal welfare of the Institute for Frontier Medical Sciences at Kyoto University.

Clinical assessment of SKG arthritis. Joint swelling was monitored by inspection and scored as follows: 0, no joint swelling; 0.1, swelling of one finger joint; 0.5, mild swelling of wrist or ankle; 1.0, severe swelling of wrist or ankle. Scores for all digits, wrists, and ankles were totaled for each mouse (12).

Antibodies. The following antibodies were used: anti-CD4 (H129.19), anti-CD8a (53-6.7), anti-CD11b (M1/70), anti-CD45RB/B220 (RA3-6B2), anti-CD49d (9C10), anti-CD106 (429), and anti-I-A/I-E (M5/114.15.2), purchased from BD Biosciences – Pharmingen (San Diego, California, USA); anti-IL-1β (AB-401-NA) (R&D Systems Inc., Minneapolis, Minnesota, USA); anti-TNF-α (L-19) (Santa Cruz Biotechnology Inc., Santa Cruz, California, USA); anti-IL-6 (D97) (Innogenetics, Gent, Belgium). For intracellular cytokine detection, the following mAb's were used: anti-IFN-γ (XMG1.2), anti-TNF-α (MP6-XT22), anti-IL-2 (JES6-5H4), anti-IL-4 (11B11), and anti-IL-10 (JES5-16E3) (BD Biosciences – Pharmingen).

RT-PCR. Total RNA was extracted from ankle joints using Isogen reagent (Nippon Gene Co., Tokyo, Japan) and reverse transcribed using Superscript II (Invitrogen Japan K.K., Tokyo, Japan). IL-1β, IL-6, or TNF-α mRNA levels were quantified by real-time PCR using QuantiTect Assay (Qiagen K.K., Tokyo, Japan) and normalized by hypoxanthine-guanin phosphoribosyl transferase (HPRT) as previously described (48). The quantities of these cytokine mRNAs were expressed as units by defining the levels of each cytokine mRNA in J774.1, a BALB/c macrophage cell line, stimulated with 1 μg/ml LPS for 24 hours, as one unit.

Histology and immunohistochemistry. Joints were fixed in 10% formalin, decalcified by 10% EDTA in PBS for 3 days, embedded in paraffin, sectioned, and stained with hematoxylin and eosin. For immunohistochemical staining, cryostat section of digits were fixed in cold acetone for 10 minutes, washed in PBS, and depleted of endogenous peroxidase by treatment with 0.3% H_2O_2 in absolute methanol for 15 minutes. After blocking nonspecific binding with 10% normal rabbit serum in PBS for 30 minutes, the sections were incubated with primary mAb's at appropriate dilutions for 1 hour at room temperature, washed, incubated with biotinylated rabbit anti-rat IgG pre-adsorbed with rabbit serum, washed and incubated with avidin-biotinylated horseradish peroxidase complex (ABC) and diaminobenzidine tetrahydrochloride (DAB) (Elite kit; Vector Laboratories Inc., Burlingame, California, USA), and counterstained with Mayer's hematoxylin.

For immunohistochemical staining of cytokines, sections were fixed for 15 minutes in ice-cold 4% phosphate-buffered paraformaldehyde (pH 7.4). The sections were then washed in HEPES-buffered saline solution (HEPES-BSS) (pH 7.1, Gibco; Invitrogen Corp., Carlsbad, California, USA) supplemented with 0.1% saponin (Sigma-Aldrich, St. Louis, Missouri, USA). All further incubations and washes were carried out using BSS-saponin. Endogenous peroxidase was inactivated by treatment with 1% formalin in BSS-saponin for 2 minutes, followed by sodium azide (0.1 M) containing 0.3% H_2O_2 for 30 minutes, blocked with 20% normal rabbit serum for 60 minutes, incubated overnight at 4°C with anti-cytokine mAb's at appropriate dilutions. The sections were then incubated with the secondary antibodies and ABC, as described above. Color was developed with AEC (DakoCytomation, Carpinteria, California, USA), and the sections were counterstained with Mayer's hematoxylin.

ELISA for autoantibody. Affinity-purified mouse IgG (5 μg/ml) and 10 μg/ml of bovine type II collagen (Funakoshi Co. Ltd., Tokyo, Japan) in PBS (pH 7.2) were used for overnight coating of ELISA plates (ICN Biomedicals Inc., Aurora, Ohio, USA). Test sera were diluted to 1:10 for anti-type II collagen antibody or 1:20 for RF assay. Alkaline phosphatase conjugated anti-mouse IgG or IgM (for RF assay) (Southern Biotechnology Associates Inc., Birmingham, Alabama, USA) was used at 1 μg/ml as the secondary reagent. Titer of RF and anti-type II collagen antibody was expressed as optical density (49).

ELISA for cytokines. The capsules of ankle joints were cut open, joint cavity was washed with 5 μl PBS, and 1 μl of withdrawn joint fluid was diluted 10-fold to assess the concentrations of IL-1β, IL-6, and TNF-α by ELISA (Biosource International, Camarillo, California, USA) according to the manufacturer's instruction, with the detection limits of 7 pg/ml for IL-1, 3 pg/ml for IL-6, and 3 pg/ml for TNF-α.

Statistics. Student's *t* test was used for statistical analyses.

Acknowledgments

This work was supported by grants-in-aid from the Ministry of Education, Science, Sports, and Culture, the Ministry of Human Welfare, and the Japan Science and Technology Agency. We thank Zoltan Fehervari for critical reading of the manuscript.

Received for publication April 5, 2004, and accepted in revised form June 29, 2004.

Address correspondence to: Shimon Sakaguchi, Department of Experimental Pathology, Institute for Frontier Medical Sciences, Kyoto University, 53 Shogoin Kawahara-cho, Sakyo-ku, Kyoto 606-8507, Japan. Phone: 81-75-751-3888; Fax: 81-75-751-3820; E-mail: shimon@frontier.kyoto-u.ac.jp.